

ALIENS, AIRCRAFT, AND ACCURACIES: SURVEYING FOR UNDERSTORY INVASIVE
PLANTS USING UNMANNED AERIAL SYSTEMS

BY

KATHLEEN A. MORAN

Bachelor of Arts, Biology, Hamilton College, 2015

THESIS

Submitted to the University of New Hampshire in Partial Fulfillment of the Requirements for the

Degree of

Master of Science

in

Natural Resources

September, 2019

This thesis was examined and approved in partial fulfillment of the requirements for the degree of
Master of Science in Natural Resources by:

Dr. Jenica M. Allen, Thesis Co-Director,
Affiliate Assistant Professor, Natural Resources & the
Environment

Dr. Russell G. Congalton, Thesis Co-Director, Professor of
Remote Sensing and Geographic Information Systems, Natural
Resources & the Environment

Heather Grybas, M.S.,
Doctoral Candidate, Natural Resources and Earth Systems Science

On June 26, 2019

Original approval signatures are on file with the University of New Hampshire Graduate School.

ACKNOWLEDGEMENTS

Thank you to Dr. Jenica Allen for taking me on as a graduate student. Your mentorship has been extremely influential in my academic and professional development, and even turned me towards my current career path (thanks, R!) You're an incredible role model. Thank you to Dr. Russell Congalton for "finding" me and sharing me with Jenica so that we could pursue this interdisciplinary project. An especially large thank you for providing the remote sensing expertise on which this project is based, and for not disowning me when I kept crashing drones. This thesis would not be what it is without the help of Ms. Heather Grybas—committee member, lab mate, and friend. I would thank you profusely for the hours you have spent helping me collect and process imagery, but instead I'll give you a lifetime pass for chorizo-based meals.

Thank you to my lab mates for making grad school far more enjoyable than expected, especially Ben Fraser, Dr. Tim Szewczyk, Rue Teel, Christine Healy, Jianyu Gu, Mitch O'Neill, Ceara Sweetser, and Linnea Dwyer. A big thank you to Dr. Tom Lee, who I greatly enjoyed teaching with and learning from these two years. Thank you to Sam Rokos for being the ultimate cat aunt and taking care of kitty through all my late nights. I also thank my parents for continuing your philosophy of "if it ain't broke, don't fix it" and generally not bothering me about school, which is the best approach you could take.

Lastly, endless thanks and love to Charles Spear for supporting (feeding) me these past two years.

This research was made possible thanks to a teaching assistantship from the Department of Natural Resources and the Environment as well as the Graduate School Summer Teaching Assistant Fellowship award.

TABLE OF CONTENTS

ACKNOWLEDGEMENTS.....	iii
LIST OF TABLES.....	vi
LIST OF FIGURES.....	vi
ABSTRACT.....	vii

CHAPTER	PAGE
I. BACKGROUND ON INVASIVE PLANTS AND REMOTE SENSING	1
<i>Invasive Plant Impacts and Management</i>	1
<i>Collecting Remotely Sensed Data</i>	4
<i>Remote Sensing Image Processing</i>	6
<i>Assessing the Accuracy of Thematic Maps</i>	9
<i>Remote Sensing of Invasive Plants</i>	10
<i>Unmanned Aerial Systems for Invasive Plant Mapping</i>	12
<i>Woody Invasive Plants in New England</i>	14
<i>Summary</i>	16
II. ALIENS, AIRCRAFT, AND ACCURACIES: SURVEYING FOR UNDERSTORY INVASIVE PLANTS USING UNMANNED AERIAL SYSTEMS.....	17
Introduction.....	17
Methods.....	21
<i>Study Area and Focal Species</i>	21
<i>Imagery Collection</i>	22

<i>Reference Data Collection</i>	24
<i>Image Processing and Classification</i>	27
Results.....	31
Discussion.....	36
LIST OF REFERENCES.....	42
APPENDIX A: Data Collection Details.....	50
<i>Site Selection and Imagery</i>	50
<i>Vegetation Plot Sampling Details</i>	53
APPENDIX B: Species-Specific Accuracy Assessment Results.....	55

LIST OF TABLES

TABLES	PAGE
1. Parameters used in Pix4D processing software that generated the highest quality orthomosaic for each season and sensor type of imagery.....	28
2. Comparison of overall (OA), user’s (UA), and producer’s accuracy (PA) for the <i>Invasive</i> class in each thematic map.....	32
3. Error matrix comparing spring RGB OBIA classification to validation reference data.....	32
4. Error matrix comparing spring RGB PBC classification to validation reference data.....	32
5. Pairwise comparison of error matrices represented by the Z statistic, generated through Kappa analysis between each pair of error matrices.....	35
A1. Phenology tracking sheet for invasive understory plants and canopy tree species.....	51
A2. Date, UAS model, camera model, sensor type, and flying height of imagery collected in 2018.....	52
A3. Ground data plot sampling field sheet used to collect validation reference data.	54
B1. Comparison of overall accuracy (OA), user’s accuracy (UA), and producer’s accuracy (PA) for classifications generated using separate <i>B. thunbergii</i> (barberry), <i>R. multiflora</i> (rose), and <i>Other</i> map classes.....	55

LIST OF FIGURES

FIGURES	PAGE
1. Study site location in New Hampshire with inset showing mission block in Mission Planner.....	24
2. Sampling design of validation data.....	25
3. Schematic of a 3 m radius plot with 1 m ² nested subplots used to characterize canopy and vegetation for validation data.....	27
4. Imagery of study area and corresponding classifications.....	33
5. Example of an <i>Other</i> plot, containing a collection of pixels totaling 28.27 m ² in area.....	34

ABSTRACT

ALIENS, AIRCRAFT, AND ACCURACIES: SURVEYING FOR UNDERSTORY INVASIVE PLANTS USING UNMANNED AERIAL SYSTEMS

by

Kathleen A. Moran

University of New Hampshire, September 2019

Invasive (alien) plants are introduced species that can cause harm to native ecosystems, industries, or human health. Managing invasive species requires knowing where they are, and early detection of new populations increases the likelihood of local eradication. Unmanned aerial systems (UAS) are an emerging remote sensing technology that can capture very high spatial resolution imagery, are easily deployed, and may offer a more efficient alternative to extensive ground surveys to locate invasive plants. Imagery collected with UAS has been used to map invasive plants in open canopy habitats, but has yet to be tested for mapping invasive plants in forest understories. My aim was to explore the feasibility of UAS as an understory invasion monitoring tool, including tests of season, sensor type, and image classification method for reliable invasive detection. I collected imagery from a 21-hectare mixed and deciduous New Hampshire forest during spring and fall periods of phenology mismatch between native vegetation and two focal invasive plants, *Berberis thunbergii* (Japanese barberry) and *Rosa multiflora* (multiflora rose). I achieved up to 82% classification accuracy by grouping *B. thunbergii* and *R. multiflora* as an *Invasive* class. There were no significant differences in

invasive detectability between sensors or classification methods, but spring imagery yielded the highest accuracies overall. Simpler pixel-based classifications are sufficient for achieving over 70% classification accuracy, though object-based segmentation can improve accuracy. UAS are promising technology with potential to reduce and target invasive plant ground surveys for temperate forest management.

CHAPTER I: Background on Invasive Plants and Remote Sensing

Invasive Plant Impacts and Management

Invasive (alien) plants are non-native species that cause ecological or economic harm to their new ecosystems (Executive Order 13112, 1999). Many invasive plants are escaped ornamental species, while others were introduced accidentally through contaminated seed or soil (Lehan et al., 2013; Reichard and White, 2001). Once introduced, if a plant thrives under its new conditions, the species can establish and spread, with varied consequences. Invasive plants can have scale-dependent effects on native vegetation richness, diversity, and evenness (Hejda et al., 2009; Powell et al., 2013; Pyšek et al., 2012; Vilà et al., 2011), and threaten rare native plant species (Farnsworth, 2004). They can also accelerate carbon and nitrogen cycles (Ehrenfeld, 2003; Liao et al., 2008) and decrease the fitness and abundance of native wildlife, particularly birds and insects (Ballard et al., 2013; Schirmel et al., 2016; Vilà et al., 2011). Invasive plants cause negative ecological impacts throughout entire ecosystems, which impairs important ecosystem services (Vilà et al., 2011).

Changes caused by invasive plants negatively affect multiple industries, including agriculture, forestry, transportation, and recreation (Eiswerth et al., 2005; Lym and Nelson, 2000; Martin and Blossey, 2012; Pimentel et al., 2005). Impacts are largely represented by control costs and product losses, yet also include other effects that are less quantifiable. In 2005, the estimate for annual crop losses and control costs for invasive weeds in the U.S. was \$27 billion dollars (Pimentel et al., 2005). One example is *Berberis vulgaris* (European barberry), which serves as a host for *Puccinia striiformis* (stripe rust), a fungus that causes yield losses of up to 25% in cereal crops (Wellings, 2011). Invasive shrubs can also inhibit regeneration of tree

seedlings by more than 200%, and they hinder forestry surveys and movement of harvesting equipment through forests (Binggeli, 2001; Fagan and Peart, 2004; Ward et al., 2018). Furthermore, the transportation industry incurs control costs through mechanical and herbicidal management of railroad and roadside infestations (Lommen et al., 2018; Lym and Nelson, 2000). Lastly, outdoor enthusiasts negatively regard invasive plants, because dense vegetation typical of some invasive plants hinders movement over terrain (Binggeli, 2001). When people are unenthusiastic about trail conditions, the recreation industry experiences financial losses (Eiswerth et al., 2005). Considering all the sectors impacted, there is strong financial and ecological incentive to better manage current plant invasions and minimize future ones.

Invasive plants also pose risks to human health. Some species are toxic, while others increase habitat for disease-carrying vectors (Derraik, 2007; Elias et al., 2006; Williams et al., 2009). The sap of *Heracleum mantegazzianum* (giant hogweed) can cause severe blisters and even blindness (Derraik, 2007), while *Ambrosia artemisiifolia* (ragweed) causes allergies throughout North America and Europe (Heberling and Fridley, 2013; Richter et al., 2013). There are approximately 300,000 cases of Lyme disease each year in the U.S. (Nelson et al., 2015), and *Berberis thunbergii* (Japanese barberry), a woody invasive shrub, provides habitat for Lyme-carrying *Ixodes scapularis* (“black-legged” or “deer” ticks) and their rodent hosts (Elias et al., 2006; Williams et al., 2009). Forest plots with invasive plants such as *B. thunbergii* have twice as many adult *I. scapularis* as plots with native-only vegetation. Similarly, Allan et al. (2010) found that removing *Lonicera maackii* (Amur honeysuckle) decreases occurrences of *Ehrlichia* disease by reducing browse for deer, which carry the host vector for *Ehrlichia*, *Amblyomma americanum* (“lone star tick”). Tick-borne diseases are expected to increase across North America and Eurasia (Ostfeld and Brunner, 2015), making invasive plant management critical.

Accurate location information is necessary for every stage of invasive plant management. Prevention is the most effective strategy for mitigating the effects of invasive species, but new introductions are inevitable (Hulme, 2006). Early Detection and Rapid Response (EDRR), in which invasive plants are located and removed shortly after entering a new area, is the next line of defense (Hulme, 2006; Westbrooks, 2004). The sooner a plant is detected, the greater the likelihood for eradication and minimization of impact (Leung et al., 2002). Once a species has become widespread and eradication is not feasible or justifiable, management strategies focus on containment by monitoring for plants that have spread beyond their accepted locales (Hulme, 2006). Distribution models of invasive species are useful for predicting future invasions at a regional scale, but targeted local monitoring is still necessary for both EDRR and containment (Allen and Bradley, 2016).

Ground surveys are an important component of invasive plant management because they confirm or deny the presence of targeted species at local scales. However, professional ground surveys are time consuming and therefore expensive. While citizen scientists are valuable for many invasive plant projects, they might overlook invasive species that would otherwise be obvious to professionals, or misidentify species (Bois et al., 2011; Jordan et al., 2012). Furthermore, recruiting, training, and organizing volunteers to survey can cost more than paying staff to accomplish the same task (Graff, 2006). As a result, if resources are limited, ground surveys should be prioritized for areas that have the highest local invasion risk. To determine those priorities, precursory exploration of an area is required to target suspect locations, and remote sensing is an attractive option to bridge the gap between regional models and ground surveys.

Collecting Remotely Sensed Data

Remote sensing is the process of gathering data about objects or landscapes without being in physical contact with them (Jensen, 2016). The advantages of remotely sensed imagery include capture of a synoptic landscape view, large spatial coverage, and in the case of multispectral sensors, detection of wavelengths not visible to the human eye (Jensen, 2016). Three major platforms are used to collect digital imagery today: satellites, manned aircraft, and unmanned aerial systems (UAS). Sensors on remote platforms vary in spatial, spectral, radiometric, and temporal resolution, as well as image extent (Bradley, 2014; Jensen, 2016).

Spatial resolution refers to the pixel size of the imagery, also known as the ground sampling distance. Landsat Thematic Mapper (TM) satellite imagery has a spatial resolution of 30 m, while commercial satellite imagery has spatial resolutions of up to 0.5 m. Aerial imagery can have a spatial resolution that ranges from multiple meters to less than 1 m, similar to commercial satellite imagery. UAS currently offer the highest spatial resolution with pixels as small as 1 cm, depending on the height at which the imagery is captured (Bradley, 2014; Whitehead and Hugenholtz, 2014; Jensen, 2016).

Spectral resolution describes the number and width of the wavelength bands detected by the sensor (Jensen, 2016). In vegetation monitoring, normal color (red, green, blue bands, or RGB), multispectral, or hyperspectral sensors are used. Normal color detects bands in the visible light spectrum and can be used to detect vegetation because chlorophyll in plants absorbs red wavelengths and reflects green wavelengths. Consequently, healthy vegetation has high reflectance in the green band and low reflectance in the red band (Jensen, 2016). Multispectral sensors detect two or more normal color (usually red and green) bands as well as bands in the near infrared (NIR), middle infrared (MIR), thermal infrared (TIR), and/or red-edge range, which can

provide information on vegetation type and stress (Li et al., 2013; Whitehead and Hugenholtz, 2014). Hyperspectral sensors collect data in hundreds of narrow bands across a continuous spectrum, which can be used to create representative signatures for particular plant species (Jensen, 2016). Spectral bands are commonly analyzed in combinations known as indices to provide additional information in the imagery. The green chromatic coordinate (GCC) index can measure the relative greenness in imagery by normalizing the green band by the RGB bands with the formula $GCC = \text{Green} / (\text{Red} + \text{Green} + \text{Blue})$ (Leduc and Knudby, 2018). The Normalized Difference Vegetation Index (NDVI), calculated using the formula $NDVI = (\text{NIR} - \text{Red}) / (\text{NIR} + \text{Red})$, is useful for assessing vegetation health, as well as discriminating between land cover types (Jensen, 2016; Li et al., 2013).

Platforms also vary in temporal resolution, or how frequently a sensor revisits a designated location (Jensen, 2016). Satellites are limited by their orbits, while manned and unmanned aerial flights can be deployed as needed, as long as weather and funding allow. Landsat 8 orbits over the same area only once every 16 days (USGS, 2016). Commercial satellite sensors can be pointed to capture off-nadir imagery of a specific location, but are still restricted by their orbits. While manned aerial flights are theoretically deployable at short notice, government-provided aerial imagery such as NAIP is only collected once every five years, and contracted aerial imagery is expensive (Bradley, 2014; Jensen, 2016). Out of all the remote sensing platforms, unmanned aerial systems (UAS) are capable of the highest temporal resolution, and can be deployed any time that flying conditions are safe and government regulations are heeded (FAA, 2017). Once imagery is collected, it can be processed into information products.

Two other ways in which remote sensing systems can differ are radiometric resolution and extent. Radiometric resolution refers to the sensitivity of the sensor to varying intensities of

reflectance (i.e., how many different shades of grey it can distinguish). Most sensors, whether satellite or UAS, collect data in either 8-bit or 16-bit storage formats. Eight-bit resolution can distinguish 256 shades of grey for each band sensed. At present, 12-bits or 4,096 shades is the maximum data a sensor can collect, which still requires the use of 16-bit storage (Jensen, 2016). Sensors also vary in the area they can capture in a single image, called the extent or footprint. Many satellite sensors can capture hundreds to thousands of square kilometers in one scene, while a single UAS flight under FAA part 107 is restricted by a 400m flying height, maintaining line of sight with the UAS, and limited battery life (FAA, 2017). However, UAS can cover numerous square kilometers of area when flown in successive missions (Fraser and Congalton, 2018), or if exemption from FAA part 107 rules is granted (FAA, 2017).

Remote Sensing Image Processing

Remotely sensed imagery can be classified, or labeled, into thematic maps showing the location and extent of user-defined classes (Lillesand et al., 2015). First, a classification scheme is defined. Classification schemes must be hierarchical, totally exhaustive, and mutually exclusive in order to label every thematic class within an image (Congalton and Green, 2019). Users may choose a pre-existing land cover classification scheme or a custom classification scheme to meet the needs of a particular project (Jensen, 2016). Once the classification scheme is clearly defined, the imagery is processed into a final map. For digital imagery, classification is mainly performed using digital image processing software such as ERDAS Imagine (Hexagon, Norcross, GA, USA), but manual image interpretation is still an option. An analyst manually interprets imagery using the elements of image interpretation: size, shape, texture, pattern, shadow, tone, and site (Jensen, 2016). Manual image interpretation is the original means of

classifying imagery, which relies on the interpreter's knowledge of an area and potential land cover types or species. Because it is limited to what the eye can see, manual image interpretation is limited in terms of distinguishing vegetation types (Jensen, 2016).

Image processing software labels imagery based on spatial and spectral pattern recognition, which incorporates a defined number of bands in the imagery and groups similar pixels (Lillesand, 2015). The two primary methods of classification are pixel-based classification (PBC) and object-based image analysis (OBIA) (Blaschke, 2010). PBC labels individual pixels based on their reflectance values across the imagery bands, and it can be either supervised or unsupervised. Supervised PBC uses training data, which are areas of the image where the land cover types are known, in order to create data representative of each map class in an image. Unsupervised PBC classification clusters pixels into groupings purely on spectral response given a user-specified number of map classes, and it is up to the user to subsequently label those groupings (Jensen, 2016).

Object-based image analysis (OBIA) has outperformed PBC in a number of studies, particularly when classifying high and very high resolution imagery (Mafanya et al., 2017; Yu et al., 2006). OBIA works by first segmenting the imagery, or grouping pixels into homogenous polygons called objects, prior to classification, mimicking the manual image interpretation process (Blaschke, 2010). Multi-scale segmentation is a common segmentation approach, which works by sequentially and repeatedly dividing the image into smaller and smaller objects (Kim et al., 2011). Multiresolution Segmentation (MRS) is a frequently used segmentation algorithm proprietary to eCognition software (Trimble, Westminster, CO). MRS first requires parameterization of scale, which determines the spectral heterogeneity of the resulting objects. A high scale parameter means that a high level of heterogeneity is allowed within objects, meaning

larger objects composed of more pixels (Baatz and Schäpe, 2000; Drăguț et al., 2014). Other built-in MRS parameters are shape and compactness (Lu and He, 2017), which are typically adjusted along with scale using a supervised, trial and error approach, until the segments satisfactorily match known classes in the imagery (Duro et al., 2012; Gao et al., 2011; Grybas et al., 2017). Automated parameterization is possible, however, and a growing movement (Drăguț et al., 2014; Grybas et al., 2017).

Once segmented, objects can be classified by a variety of algorithms, including machine learning. Machine learning is a growing subset of classification methods, and includes Support Vector Machines (SVM), and Random Forest (RF) algorithms (Blaschke, 2010; Burges, 1998; Husson et al., 2016). SVM is a supervised, binary classification method, which uses training data to build a model, set a threshold or hyperplane, and then label validation samples based on whether they exceed that threshold or not (Tzotsos and Argialas, 2008). Despite the required extra computing steps, this method is highly regarded for land cover classification due to its ability to incorporate a large number of input variables. For OBIA, there can be many different variables, such as object size, shape, and heterogeneity, along with spectral values (Tzotsos and Argialas, 2008). Random Forest is also used for land cover classification and utilizes decision trees to determine the optimal class label (Jensen, 2016). OBIA and machine learning methods are increasingly used for high resolution imagery classification, but PBC methods are more accessible to a wider audience. Open source PBC software such as MultiSpec, with accompanying user guides (Purdue Research Foundation, 2019), enable users with limited training to apply PBC techniques.

Assessing the Accuracy of Thematic Maps

Accuracy assessment quantifies the quality of a thematic map by comparing classified samples to validation reference data (Congalton and Green, 2019). Validation data are samples labelled with the correct class for each land cover type, although there is always some degree of uncertainty and thus these samples cannot be referred to as “ground truth.” Validation data can be collected on the ground, interpreted from higher resolution imagery, or extracted from pre-existing maps. There are a number of important considerations when deciding the size of the sample unit with which to collect validation data. One must consider the minimum mapping unit (MMU), or smallest mapped element, and the positional accuracy of the resulting thematic map (Congalton and Green, 2019). The sample unit size used for validation data must be large enough to encompass the MMU, often 3 pixels by 3 pixels, while also accounting for positional error. The analyst must be confident that every validation sample unit overlaid on a thematic map encompasses the intended area, allowing for a direct comparison between thematic and validation classes. The comparison of thematic map to validation data results in an error matrix, which serves as the basis for quantitative assessment of classification accuracy (Congalton and Green, 2019).

An error matrix, or contingency table, is a cross-classification that tallies the agreement and disagreement between the thematic map and the validation data (Congalton and Green, 2019). Three accuracy metrics are derived from an error matrix: user’s, producer’s, and overall accuracy (Congalton and Green, 2019). User’s accuracy (UA) represents errors of commission, or how likely a map class is to be labelled in the wrong map category, while producer’s accuracy (PA) represents errors of omission, or the likelihood a map class will be excluded from the class to which it belongs (Story and Congalton, 1986). Overall accuracy (OA) is the total number of

correctly identified samples divided by the total number of discrete validation samples (Congalton, 1991). Reporting and comparing the user's, producer's, and overall accuracies between error matrices of different thematic maps is a common method for analyzing classification performance. To test whether a classification performed significantly better than random, or if one error matrix is significantly different from another, one can perform Kappa analysis (Congalton and Green, 2019). A Kappa analysis of a single error matrix indicates whether a classification was significantly better than random, while a pairwise Kappa analysis between two error matrices determines whether two error matrices are significantly different from one another (Congalton and Green, 2019). Reporting the accuracies for error matrices is still valuable, but a Kappa analysis can reveal whether one classification is significantly different from another.

Remote Sensing of Invasive Plants

The use of remote sensing provides an opportunity to enhance invasive plant monitoring and has already been used successfully in select situations. Landsat satellite imagery, with a 30 m spatial resolution, is effective for mapping some rangeland and desert invasive plants such as *Bromus tectorum* (cheatgrass) and *Pennisetum clilare* (buffelgrass) across landscapes when target species are highly abundant (Olsson et al., 2011; Singh and Glenn, 2009). High resolution satellite and aerial imagery provide the spatial resolution necessary for detecting sparser populations of invasive plant species, at a high financial cost (Müllerová, Pergl, & Pysek, 2013). Very high spatial resolution satellite imagery (Rapid Eye, 5 m) is sufficient for mapping regional levels of invasion of *Heracleum mantegazzianum* (giant hogweed) and *Fallopia spp.* (knotweed) in open canopy settings, but very high spatial resolution imagery (< 0.5 m, RGB, aerial orthophotos) is necessary for early detection and monitoring (Müllerová et al., 2017a, 2013).

Remotely sensed satellite and airborne imagery has also been used to map invasive plant species in forested landscapes. Landsat satellite imagery is adequate for identifying large extents of *Rhamnus cathartica* (common buckthorn), *Frangula alnus* (glossy buckthorn), and *Lonicera maackii* (Amur honeysuckle) in temperate forests (Becker et al., 2013; Resasco et al., 2007). Higher spatial resolution imagery, such as 0.3 m aerial orthoimagery, is necessary to map smaller incursions of understory *L. maackii* (Shouse et al., 2013). As in open settings, thematic accuracy in understory settings increases as imagery pixel size decreases, with very high resolution imagery recommended for monitoring local-scale invasions (Shouse et al., 2013). The financial cost of commercial satellite and aerial imagery, however, severely inhibits the realistic application of these methods to invasive plant management efforts, particularly EDRR.

Phenology is critical for deciding when to collect imagery for invasive plant mapping. For invasive plants in open settings, collecting imagery during flowering is ideal because that is when spectral responses are most unique (Mullerova et al., 2013). Other rangeland and desert species are best imaged and classified during early season green up or shortly after a rain event (Olsson *et al.*, 2011; Singh and Glenn, 2009). Remotely sensing understory invasive plants in deciduous forests is more difficult because the forest canopy leafs out in spring, obscuring vegetation below. However, due to asynchrony in leaf out and leaf off timing, it is possible to detect understory invasive plants in early spring or late fall if populations are sufficiently large for the sensor resolution (Resasco, 2007; Becker *et al.*, 2013). Remote detection of understory invasive plants remains comparatively underutilized due to lack of affordable, accessible, and timely very high spatial resolution imagery, but UAS provide a means to quickly collect detailed imagery during brief phenological windows.

Despite success using satellite and aerial imagery to map invasive plants, the spatial and temporal resolution may be too coarse or the costs too high for certain applications (Bradley, 2014). Landsat imagery is free, but the 30 m resolution can only detect large extents of invasive plants (Jensen, 2016). Commercial 1 m resolution imagery, such as GeoEye-1, shows much more detail, but costs thousands of dollars per scene and is therefore not practical for tracking phenological changes across numerous dates (Bradley, 2014). Furthermore, specific scenes of commercial satellite imagery must be ordered ahead of time and are limited temporally by orbits (Bradley, 2014). For collecting imagery of understory invasive plants during canopy leaf-off, there is a short phenological window that varies from year to year that could easily be missed if relying on satellite imagery. EDRR and containment rely on being able to find small clusters of unwanted plants before they become widespread. Therefore, in order for remote sensing to be a viable monitoring tool, the system must have a high spatial resolution (< 1 m) to detect individual plant patches or shrubs, be relatively inexpensive, and be easily deployable.

Unmanned Aerial Systems for Invasive Plant Mapping

UAS provide an opportunity to resolve many previous issues with remote detection of invasive plants. UAS can be deployed with high temporal frequency on a flexible schedule to take advantage of short phenological windows needed to differentiate target species from surrounding vegetation (Mullerova et al., 2017b). UAS can support a variety of sensors, and even the most inexpensive UAS have spatial resolution superior to commercial satellite imagery. The result of higher resolution is less spectral mixing per pixel, which should aid in detecting small groups of plants instead of large infestations. One of the most expensive components to UAS are high accuracy GPS units, which use real time kinematic (RTK) or post processing kinematic

(PPK) corrections to differentially correct GPS coordinates of the imagery using a known base station (Whitehead and Hugengoltz, 2014). High GPS accuracy is important for research to ensure low positional error, but lower cost moderate GPS accuracy (5-10 m) may be sufficient for locating areas for targeted ground surveys. When considered on a per-use cost, UAS are more economical than commercial or commissioned imagery, even when adding in the cost of processing software (Bradley, 2014; Mullerova et al., 2017b; Whitehead and Hugengoltz, 2014). The cost of one moderately priced UAS is approximately the same as ordering 1-3 scenes of commercial satellite imagery, but the UAS can be deployed to collect imagery repeatedly (Bradley, 2014; Whitehead and Hugengoltz, 2014). For purposes such as monitoring, especially in phenologically sensitive systems with annual variability in leafing transition dates, a remote sensing system that can be deployed at a moment's notice and numerous times in a single week is advantageous.

One unique advantage that UAS imagery has over satellite sensing platforms is Structure from Motion (SfM). SfM is achieved by collecting imagery with high levels of overlap, which can then be relatively positioned based on common key points between numerous images (Dandois and Ellis, 2013). The overlap allows the creation of point clouds, and while not a direct substitute for LiDAR, they can be used for height models that are particularly helpful in classifying forest vegetation (Lefsky et al., 2002). Using SfM, UAS imagery can be separated into canopy points and understory points. By filtering out canopy points, the understory vegetation points remain, which can lead to higher invasive plant detection accuracies (Leduc and Knudby, 2018). When SfM is combined with high accuracy image geotagging, this results in a georeferenced orthomosaic from which measurements can be made (Dandois and Ellis, 2013).

Woody Invasive Plants in New England

New England is a heavily forested and heavily invaded landscape with active invasive plant management programs. Woody shrubs are the dominant invasive flora of New England (Bois et al., 2011; Lehan et al., 2013) and most were first introduced as landscaping or erosion control plants and subsequently expanded beyond their intended confines (Lehan et al., 2013; Reichard and White, 2001). Infrastructure, particularly roads, as well as forest fragmentation have assisted in the spread of woody invasive plants by creating disturbance and/or microclimate variation at forest edges (Allen et al., 2013; Brothers et al., 2009; Christen and Matlack, 2009; Matlack, 1993). Invasive plants can take advantage of edge effects, and frequently establish on forest peripheries and migrate into the interior (Brothers et al., 2009). Most woody invasive plants in New England are able to establish in new areas quickly due to common invasive traits: invasive elsewhere in the world, fast growth rate, and a match of their native latitudinal range to New England (Herron et al., 2007).

Some woody understory invasive plants also exhibit extended leaf phenology (ELP), which enables them to have a longer growing season than native tree and understory species (Dreiss and Volin, 2013; Fridley, 2012; Smith, 2013). Invasive plants with ELP can leaf out earlier and/or hold their leaves longer into fall than natives, which can lead to more growth and better establishment (Smith, 2013). While ELP understory species overall have a longer growing season than northeastern canopy species, asynchrony is a complex dynamic that varies by season and species (Fridley, 2012; Dreiss and Volin, 2013). Native trees vary in phenology, with *Acer* species leafing out early, and *Quercus* and *Fagus* species holding their leaves later in the fall and sometimes well into winter (Kosmala et al., 2016; Otto and Nilsson, 1981; Richardson et al., 2006).

Berberis thunbergii (Japanese barberry) and *Rosa multiflora* (multiflora rose) are common woody invaders of northeastern temperate forests (USDA, 2018; Fridley, 2012). *Berberis thunbergii* originated in Asia and was introduced to the U.S. as an ornamental, and is desirable for landscaping because thorns make it resistant to deer grazing and it overwinters well (USDA, 2018). *Rosa multiflora* also originated in Asia and was popularly used to create hedgerows due to its height of up to 6 ft and dense growth habit (USDA, 2018). It is a common invader of roadsides, which facilitate the spread of the shrub (Christen and Matlack, 2009; Flory and Clay, 2006) and can tolerate a range of light and soil fertility conditions within temperate deciduous forests (Dlugos et al., 2015; Huebner et al., 2014). Both *B. thunbergii* and *R. multiflora* exhibit ELP which results in increased carbon gain in spring for *B. thunbergii* and fall for *R. multiflora* (Dlugos et al., 2015; Fridley, 2012; Polgar et al., 2014). Both shrubs leaf out earlier than other native and woody invasive species, making them ideal candidates for early spring imagery collection with UAS. *Berberis thunbergii* and *R. multiflora* are not EDRR species because they are abundant across the Northeast, but they are actively managed for containment.

Summary

Invasive plants negatively affect numerous facets of society and nature, with substantial environmental, economic, and human health costs. Woody invasive plants are particularly abundant in temperate deciduous forests of the northeastern U.S., due in part to extended leaf phenology. The asynchrony between native canopy and understory invasive species provides the opportunity to use remote sensing for invasive plant surveys during periods of canopy leaf off. Unmanned aerial systems offer high spatial and spectral resolution, relatively low cost, and quick deployability. The resulting imagery can be compiled into detailed, classified maps showing the locations of target species. These maps would allow land managers to better focus their invasive plant control efforts, and allow for more time managing infestations, rather than searching for them on the ground.

CHAPTER II: ALIENS, AIRCRAFT, AND ACCURACIES: SURVEYING FOR UNDERSTORY INVASIVE PLANTS USING UNMANNED AERIAL SYSTEMS

INTRODUCTION

Invasive plants are non-native species that cause ecological or economic harm in their recipient ecosystems (Executive Order 13112, 1999). The negative impacts of invasive plants influence multiple industries, including agriculture, forestry, transportation, and conservation (Eiswerth et al., 2005; Lym and Nelson, 2000; Martin and Blossey, 2012; Pimentel et al., 2005). Invasive plants also affect the intrinsic value of native ecosystems by accelerating carbon and nitrogen cycles (Ehrenfeld, 1997; Liao et al., 2008) and decreasing the fitness and abundance of native wildlife, particularly birds and insects (Ballard et al., 2013; Schirmel et al., 2016; Vilà et al., 2011). Additionally, invasive plants pose significant risk to human health. Some species increase habitat for disease-carrying vectors (e.g., increased Lyme-carrying ticks in invasive Japanese barberry; Williams et al., 2009), while others are toxic (Elias et al., 2006; USDA, 2018; Williams et al., 2009). In order to mitigate the detrimental effects of invasive plants, we must be able to track and manage their presence within a landscape.

Accurate location information is necessary for every stage of invasive plant management. Early detection and rapid response (EDRR), in which invasive plants are located and removed shortly after establishing in a new area, is the most effective post-introduction management strategy and requires detection of small, isolated populations (Hulme, 2006; Westbrooks, 2004). Containment aims to restrict the further spread of an already established invasive species by quickly locating and removing new incursions (Hulme, 2006). Species distribution models are useful for predicting future invasions at a regional scale, but ground surveys remain necessary for confirming identifications and removal of invasive plants (Allen & Bradley 2016). However,

professional field work is costly and while citizen scientists contribute valuable data, they may overlook new invasive species that are not yet well-known on the landscape (Bois *et al.*, 2011; Jordan *et al.*, 2012). More efficient monitoring methods can facilitate more effective invasive plant management by focusing resources on controlling plants rather than looking for them.

Remote sensing provides an opportunity to enhance invasive plant monitoring. Satellite and near surface remote sensing, such as unmanned aerial systems (UAS), have potential to expand the spatial extent and/or temporal frequency of invasive plant monitoring compared to ground surveys. Publicly available satellite imagery (e.g., Landsat, MODIS) provide multispectral imagery with extensive spatial coverage, but they have medium to coarse spatial and temporal resolution. This imagery is useful in some cases for mapping expansive coverages of invasive plants, particularly rangeland and desert plants (Olsson *et al.*, 2011; Singh and Glenn, 2009). Very high resolution (0.5 m) satellite imagery has been successfully used to map regional invasions (e.g., giant hogweed), but is not optimal when trying to quickly collect data during short phenological windows (Mullerova *et al.*, 2017b).

UAS provide a unique opportunity for understory invasive plant monitoring due to their capability for very high spatial, spectral, and temporal resolution. UAS can be piloted from the ground both manually or autonomously using mission planning software (Whitehead and Hugengoltz, 2014). UAS can support a variety of imaging systems, including red-green-blue (RGB) and multispectral (MSP) sensors. MSP sensors, while more expensive, are desirable for deriving vegetation indices, which can increase classification accuracy. MSP sensors are especially helpful in determining the difference between senescing and healthy vegetation which would be useful in separating invasive plants with extended leaf phenology from declining native vegetation (Bradley, 2014), Komarek *et al.* (2018) highlighted the increase in accuracy achieved

using a MSP sensor over RGB for vegetation classification from UAS imagery. However, RGB imagery has proven sufficient in detecting both native and invasive species, in addition to being less expensive than MSP sensors (Hill et al., 2017; Leduc and Knudby, 2018). Furthermore, some MSP sensors also lack sensitivity to blue bands of light (Bradley, 2014), which are helpful for cutting through shadows, common in forest understories.

Regardless of spectral resolution, even the most inexpensive UAS have spatial resolution superior to commercial satellite imagery. For example, UAS multispectral imagery outperformed WorldView 2 commercial satellite imagery (2 m spatial resolution, multispectral) in mapping *Robinia pseudocaccia* (invasive black locust tree, Mullerova et al. 2017a). In addition to high spatial resolution, UAS can be deployed as needed to capture short phenological windows critical for differentiating species (Bradley and Mustard, 2006; Mullerova et al., 2017b). When considered on a per-use cost, UAS are more economical than commercial or commissioned imagery, and they can be deployed more frequently (Bradley, 2014; Mullerova et al., 2017b; Whitehead and Hugengoltz, 2014).

Detection of forest understory invasive plants pose unique challenges due to the forest canopy cover above them. The leaves in the canopy are a physical barrier against capturing understory imagery for the majority of the growing season, but short windows of phenological mismatch provide some opportunity for understory invasive plant imaging. Asynchronous phenology refers to understory invasive plants in temperate forests leafing out earlier and/or dropping leaves later than native understory plants and canopy trees (Dreiss and Volin, 2013; Fridley, 2012). The relative phenologies of different species in deciduous forests provide a short temporal window in spring and fall for mapping using remote sensing, in which the canopy is largely open, but invasive plants below are in leaf-on stage. Most remote sensing studies have

focused on species that hold their leaves long into fall. *Rhamnus cathartica* (common buckthorn), *Frangula alnus* (glossy buckthorn), and *Lonicera maackii* (Amur honeysuckle) are invasive species that exhibit fall extended leaf phenology, and expansive populations have been identified using Landsat scenes (Resasco, 2007; Shouse *et al.*, 2013). However, high resolution imagery is more accurate for mapping at a local scale (Becker *et al.*, 2013) and, we expect, for lower density and small populations. There are also a number of understory invasive species that leaf out early in spring, such as *Berberis thunbergii* and *Rosa multiflora* (Polgar *et al.*, 2014). There have not yet been any remote sensing studies—satellite or UAS—on the best season to detect these species. Overall, UAS provide the quick deployment and high spatial resolution needed to detect individual plant patches or shrubs in short windows of asynchronous phenology, yet their efficacy in mapping understory invasive plants has not yet been tested.

Object-based image analysis (OBIA) methods are growing in frequency amongst high spatial resolution remote sensing studies (Blaschke, 2010; Komárek *et al.*, 2018; Lu and Weng, 2007), but they may not be the best classification method for every situation. OBIA classification requires either expensive segmentation software and an analyst trained in using it, or an analyst with programming knowledge to run models in open source settings. If UAS are to be a widely applied management tool, users must be able to effectively analyze the imagery. Pixel-based classification (PBC) methods are generally simpler and available through open source software (e.g., MultiSpec, 2018). On occasion, simple pixel-based classifications (PBC) such as Maximum Likelihood have even outperformed sophisticated machine learning OBIA methods (Mullerova *et al.*, 2017b). There is a possibility that PBC may outperform OBIA understory classification if vegetation shapes are indistinct and pixelated, in which case the additional information provided by OBIA may not be beneficial.

I aimed to test the feasibility of using UAS for understory invasive plant mapping in temperate deciduous forest. Using imagery collected in spring and fall, and with RGB and multispectral sensors, I focused on mapping two woody invasive species common to New England forests that exhibit extended leaf phenology to ask 1) how accurately can understory invasive plants be detected? and 2) what sensor type, season, and classification method produce the most accurate detections? Identifying the capabilities and limitations of using UAS to map invasive understory plants will guide recommendations for the adoption of this emerging technology by land managers looking for more efficient ways to manage invasive plants.

METHODS

Study Area and Focal Species

The study area is a 750 m x 300 m site located at Kingman Farm, a part of the University of New Hampshire (UNH) Agricultural Experiment Station in Madbury, NH. The site is completely forested with deciduous and mixed stands, which provide seasonal leaf cover, and appropriate adjacent launching and landing sites for UAS pursuant to FAA regulations (FAA, 2017). The understory contains populations of the target invasive plants (Appendix A), *Berberis thunbergii* (Japanese barberry) and *Rosa multiflora* (multiflora rose), both of which are widespread and common New England invasive plants (USDA, 2018) that display extended leaf phenology (Fridley, 2012).

Berberis thunbergii (Japanese barberry) is a perennial shrub that was introduced to the U.S. from Asia in the late 1800s as an ornamental and has since become invasive throughout the northeastern U.S. and Midwest (Silander and Klepeis, 1999; USDA, 2018). *Berberis thunbergii* is undesirable because it impedes recreation, increases habitat for black-legged ticks that carry Lyme disease (Williams *et al.*, 2009), suppresses native tree recruitment (Link *et al.*, 2018), and

alters microbial communities by increasing soil pH and nitrification rates (Kourtev *et al.*, 2003). *Rosa multiflora* (multiflora rose) is another introduced perennial shrub that forms dense thickets, reducing native plant species richness (Yurkonis *et al.*, 2005). Like *B. thunbergii*, *R. multiflora* is native to Asia and was introduced to the U.S. in the mid 20th century as a living fence for livestock (Evans, n.d.). It grows well in disturbed areas such as roadsides and pastures, but is also capable of thriving under closed canopy conditions (Huebner, 2003), which has led to widespread invasion across both the eastern and western U.S. (USDA, 2018). After years of being sold as an ornamental, *R. multiflora* is on the Prohibited Species List for New Hampshire (NH Dept. Agriculture, 2017) and banned in a number of other states (USDA, 2018). Control of *B. thunbergii* and *R. multiflora* is possible, but requires persistent management (Evans, 1983; Ward, 2013).

Imagery Collection

I flew two UAS for this study: a fixed wing eBee Plus (senseFly, Cheseaux-sur-Lausanne, Switzerland) and a quadcopter Eagle XF (UAV America, Nottingham, NH). The eBee Plus held two sensors: a Parrot Sequoia multispectral camera (MicaSense, Seattle, WA), consisting of green, red, red-edge, and near-infrared bands; and a 20 megapixel RGB Sensor Optimized for Drone Applications (S.O.D.A.; senseFly, Cheseaux-sur-Lausanne, Switzerland). The Eagle XF was outfitted with an a7R 36 megapixel RGB sensor (Sony, Tokyo, Japan).

Prior to collecting imagery, I set out ground control points in a defined area to mark known populations of *B. thunbergii* and *R. multiflora* for later use as classification training data. I then constructed mission plans using the flight planning software eMotion (senseFly, Cheseaux-sur-Lausanne, Switzerland) for the eBee Plus and Mission Planner (ArduPilot,

ArduPilot Dev Team v1.3, 2018) for the Eagle XF. The flight block covered the entire 750 x 300 m study area and included 85% sidelap and endlap to maximize image overlap for orthomosaic processing (Figure 1). I flew missions at heights of 80 m, 100 m, and 120 m to ensure adequate image calibration and orthomosaic creation (Table A2).

I collected normal color (RGB) and multispectral (MSP) sensor imagery in spring and fall of 2018. Spring image acquisition included six flights from 12 April 2018 to full canopy leaf out on 23 June 2018. I selected 23 April 2018 for MSP (100 m height) and 4 May 2018 for RGB (80 m height) as the best dates of spring imagery based on visual inspection of species phenology both on the ground and in the imagery (Appendix A, Table A1, Table A2). The 4 May 2018 flight covered a smaller area than the others due to a technical malfunction, resulting in 4 validation plots, *Other* and *B. thunbergii*, left uncovered by the resulting imagery. However, invasive species were most visually apparent in this date of imagery so I retained it for analysis. To account for the lost validation plots on this date of imagery, and to better balance the accuracy assessment for all dates of imagery, I augmented the original number of *Other* samples to a total of 30 for 4 May 2018 and 32 for all other dates of imagery (see *Reference Data*). I collected one date of fall imagery using both RGB (100 m) and MSP (120 m) sensors on 9 November 2018, after waiting as long as possible for adequate canopy leaf drop (Appendix A).

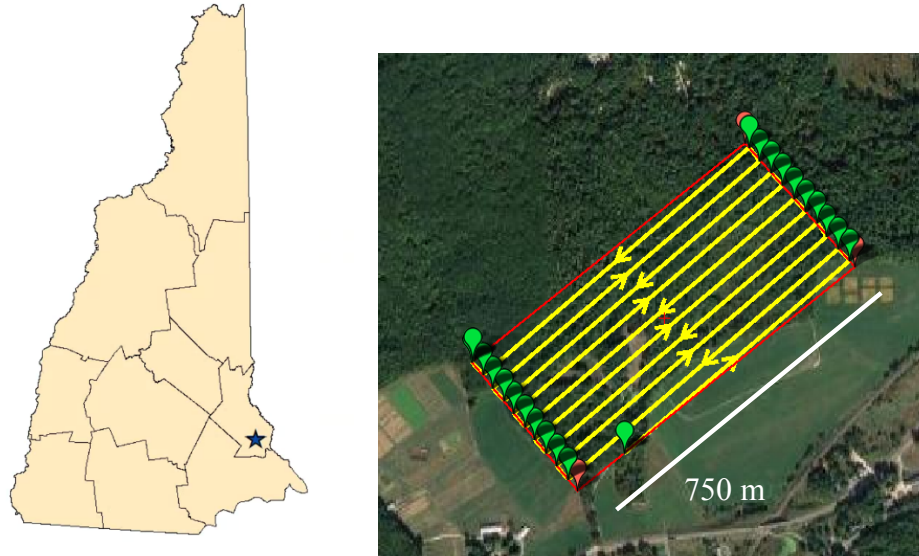


Figure 1: Study site location (star) in New Hampshire with inset showing mission block in Mission Planner. Flight block (red polygon), flight lines (yellow lines and arrows), and waypoints (green points).

Reference Data Collection

I collected training and validation reference data in July 2018 for use in later accuracy assessments. I delineated areas, “patches,” dominated by *B. thunbergii* and *R. multiflora* using waypoints taken during random haphazard surveys (Appendix A). *Berberis thunbergii* patches were mostly homogeneous, but all patches containing *R. multiflora* also contained non-dominant populations of *B. thunbergii* and other vegetation. I created polygons of each invasive plant patch in ArcMap (ESRI, Redlands, CA) by processing perimeter vertex points collected with a GPSMap76CS (Garmin, Olathe, KS; horizontal accuracy: 5-10m; coordinate system: WGS84; WAAS enabled). I delineated training data areas prior to collecting imagery, to ensure that the flight block covered an area with dominant *B. thunbergii* and *R. multiflora* for training sample selection. I set out ground control points (GCPs) around the perimeter of homogenous patches of the two invasive species, so that the GCPs would be visible in the imagery. I selected training data for the *Other* class in the vicinity of the *B. thunbergii* and *R. multiflora* training location, in

areas where I was confident on the absence of the two invasive species. I then used three *B. thunbergii* and two *R. multiflora* patches for validation data based on their proximity (within 1000 ft.) to the only feasible base station location for survey-grade GPS (Topcon HiperLite, Tokyo, Japan; 10mm Real-Time Kinematic standard horizontal accuracy; NAD83 New Hampshire State Plane coordinate system). I transformed each validation patch into a rectangular validation sampling area with a 6 m buffer to ensure validation plot locations would fall within the rectangle using the ArcMap Buffer tool (Figure 2).

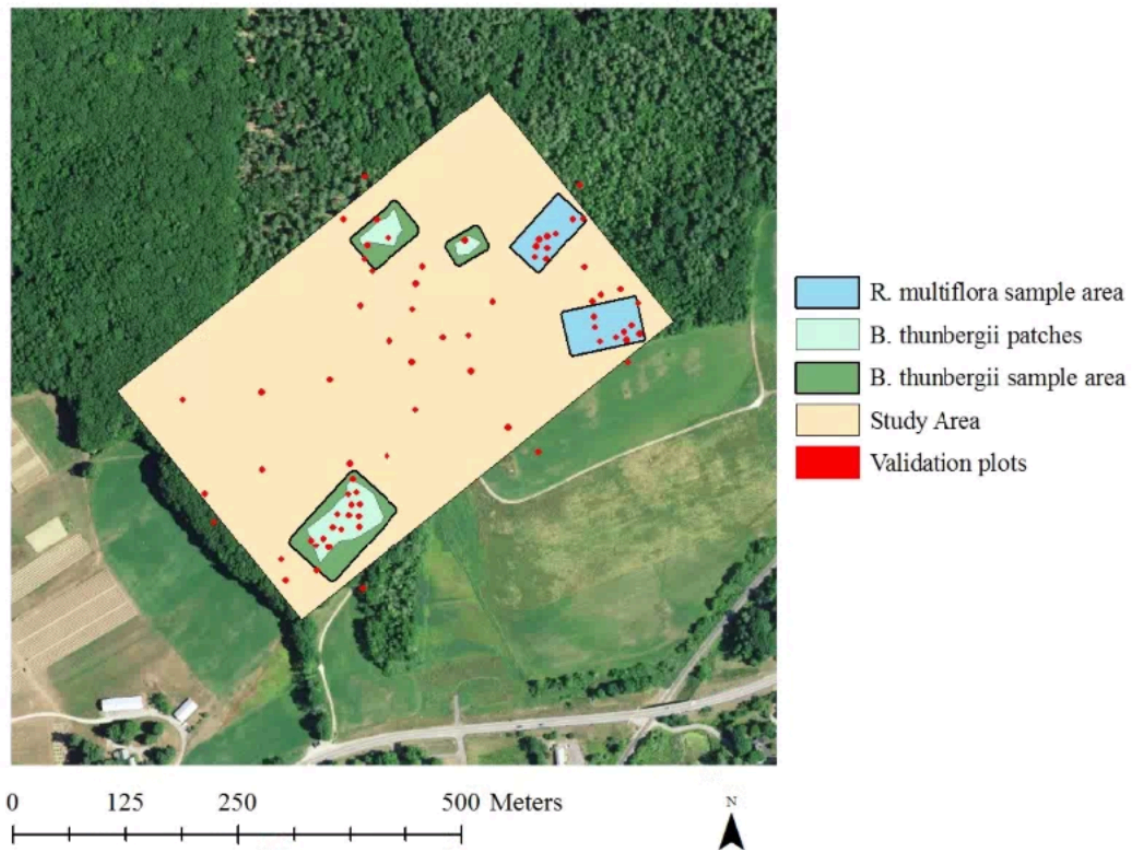


Figure 2: Sampling design of validation data. Includes patches of *B. thunbergii* and *R. multiflora* delineated using Garmin GPS and rectangular, buffered validation areas with randomly generated validation plots within each map type (20 *B. thunbergii*, 20 *R. multiflora*, and after augmentation, 32 total *Other*).

Within the buffered validation sampling areas, I generated stratified random samples for each of three map classes (*B. thunbergii* dominant, *R. multiflora* dominant, *Other*) to characterize ground vegetation to use as validation data in my classification accuracy assessments (Figure 2). I generated 20 samples to serve as validation plot locations for both the *B. thunbergii* and *R. multiflora* map classes and 10 plots for the *Other* class, for a total of 50 plots. I ensured at least a 1 m buffer between each *B. thunbergii* and *R. multiflora*-dominant validation plot. To maximize spacing between *Other* validation plots, I divided the study area into four quadrants, took the diagonal of one quadrant, and divided it into eighths. This sampling method is modified from Congalton and Green (2019) and resulted in random plots at least 38 m apart.

Additional *Other* validation plots were later chosen to augment the original samples and yield a more statistically balanced accuracy assessment. To select these samples, I generated 30 random points, at least 40 m apart, in ArcMap. Then, out of the 30 random points, I manually interpreted 22 new *Other* validation plots from the 4 May 2018 imagery. I placed plots in areas free of understory invasive species, not overlapping any areas used for *Other* training samples, and as close to the corresponding generated random point as possible. I confidently interpreted the imagery due to the high spatial resolution, clear difference in native and invasive species phenology, and my general understanding of the area. I then used the combined original and new *Other* validation plots in all accuracy assessments.

Each random plot generated within the *B. thunbergii* and *R. multiflora* validation areas represented a 3 m radius validation plot with three nested 1m² subplots (Figure 3). The purpose of the 3 m radius plots was to characterize and confirm the general vegetation composition, canopy composition and closure, and ground type within the plot (Appendix A, Table A3). I recorded the center location of each plot using a HiperLite Plus survey grade GPS system

(Topcon, Tokyo, Japan; 10mm Real-Time Kinematic standard horizontal accuracy; NAD83 New Hampshire State Plane coordinate system) fixed to a Topcon base station collecting static positional data. I estimated canopy closure using a modified Braun-Blanquet scale, with categories of <5%, 5-25%, 25-50%, 50-75%, and 75-100%. I also recorded composition (e.g., 75% red maple, 25% black birch), and included all trees and saplings taller than 2 m. I visually estimated the total percent coverage of understory vegetation in the plot, as well as *B. thunbergii*, *R. multiflora*, herbaceous, shrub, and fern coverage using the same modified Braun-Blanquet scale. Other physical and ecological data that might affect classification accuracy were also collected, including density in the 1 m² subplots, but not used in data analysis (Appendix A).

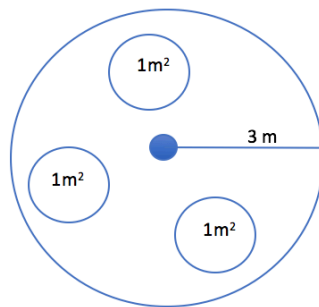


Figure 3: Schematic of a 3 m radius plot with 1 m² nested subplots used to characterize canopy and vegetation of each stratified random sampling location used for validation data.

Image Processing and Classification

I processed imagery using Pix4D software (senseFly, Cheseaux-sur-Lausanne, Switzerland) to create georeferenced orthomosaics of the study area. To ensure high positional accuracy of the resulting models, I Post-Process Kinematic (PPK) corrected the GPS-tagged imagery using the local NHUN Continuously Operating Reference Station (CORS) (National Geodetic Survey, 2018; Pix4D, 2018). There are a number of orthomosaic processing options

within Pix4D, notably keypoints image scale, point cloud image scale, point cloud density, 3D textured mesh resolution, and sample density divider (Pix4D, 2018). I selected optimal settings for each date of imagery (Table 1) based on systematic trial and error and assessment of the number of calibrated images and point cloud density (Pix4D, 2018), as well as qualitative visual assessment of the resulting orthomosaic models.

Table 1: Parameters used in Pix4D processing software that generated the highest quality orthomosaic for each season and sensor type of imagery. Additional settings included point density (high), 3D Textured Mesh (high resolution), geometrically verified matching, and no surface smoothing, which remained constant across models.

Season	Sensor	Keypoints Image Scale	Point Cloud Image Scale
Spring	RGB	1	1/2
Spring	MSP	1	1/4
Fall	RGB	1	1/2
Fall	MSP	1	1/4

For each of the resulting orthomosaics, I also created additional vegetation indices in R 3.5 (R Core Team, 2018). For RGB imagery, I calculated the Green Chromatic Coordinate (GCC), which measures the relative greenness in an image and is helpful in distinguishing vegetation types, calculated by $GCC = \text{Green} / (\text{Blue} + \text{Green} + \text{Red})$ (Harris Geospatial, 2017; Leduc and Knudby, 2018). I calculated a Normalized Difference Vegetation Index (NDVI) for each MSP orthomosaic, calculated by $(NIR - \text{Red}) / (NIR + \text{Red})$, which is sensitive to stages of plant health and is useful in vegetation classification (Jensen, 2016). I experimented with a number of other vegetation indices but ultimately selected GCC and NDVI due to their ability to increase separation between training data spectral responses.

I performed supervised pixel-based (PBC) and object-based image analysis (OBIA) classifications on each of the final orthomosaics to determine which provided the most accurate maps of the target invasive species. For PBC, I used a maximum likelihood classification

algorithm for spring imagery and non-parametric parallelepiped for fall in ERDAS IMAGINE (Hexagon Geospatial, Madison, AL, 2018). Parallelepiped classification uses the outer bounds (i.e., minimum and maximum) of the training data pixel values to determine whether unclassified pixels fall in—and will be labeled with the training data class—or out. Using the maximum likelihood algorithm for the fall imagery would have been ideal, but because training samples were highly heterogeneous and not invertible, I was unable to calculate necessary sample statistics (ERDAS IMAGINE, 2018). For spring imagery, I used the region growing tool to select training data samples, which expands a region of neighboring pixels within a designated Euclidean distance threshold (ERDAS IMAGINE, 2018). I was unable to use the region growing tool with the fall imagery, and instead selected polygonal training samples where the understory was visible, which was different in some cases from the spring training samples. For each PBC classification, I selected at least 10 training samples comprised of no less than 20 pixels for both *B. thunbergii* and *R. multiflora* invasive classes using areas of vegetation in the training ground data area that I was confident on vegetation species. I also visually selected at least 10 samples of no less than 20 pixels for each of the following classes: deciduous tree canopy, tree stem, leaf litter, grass, skunk cabbage, water, and bare ground which I later collapsed into *Other* following classification.

After running the supervised, PBC classification, I applied a 3 x 3 majority filter on the 3 cm spatial resolution RGB spring and fall imagery to achieve a spatial resolution comparable to the 13 cm resolution of the spring and fall MSP imagery. Then, I performed the accuracy assessment with a minimum mapping unit (MMU) of 1 m², where each classified plot needed at least 1 m² of invasive species in order to be considered *Invasive*, otherwise it was *Other*. The MMU of 1 m² covers the growth habit of both *R. multiflora* and *B. thunbergii*, while filtering out

false positives for invasives that may otherwise occur due to chance with a much smaller MMU. Both the MMU of 1 m² and the 3 m radius validation plot account for the horizontal positional error of the orthomosaics (all RMSE < 0.3 m) and the GPS unit (<0.1 m).

OBIA classification first segments imagery into homogenous polygons, which are then labeled based on spectral and spatial properties (Blaschke, 2010). I performed Multiresolution segmentation (MRS) for each orthomosaic in eCognition (Trimble, Westminster, CO) using an iterative qualitative approach, choosing optimal parameters as those that resulted in segmentation that most resembled the natural shape of objects in the imagery. The major parameters determining segmentation are shape, scale, and compactness. For RGB imagery, a scale of 30, shape of 0.1, and compactness of 0.1 yielded optimal segmentation. For MSP imagery, parameters scale: 30, shape: 0.5, and compactness: 0.5 were optimal. Following segmentation, I selected and labeled at least 10 training data objects for each class from within my known ground data training area and ran a Support Vector Machine (SVM) classification in eCognition (Trimble, Westminster, CO). I used the following object variables in the SVM: means and standard deviations for each band and index, brightness, pixel area, roundness, and compactness. SVM, a supervised machine learning method, has been used to classify vegetation types down to individual species from UAS collected imagery (Komarek *et al.*, 2018). I ran the SVM classification numerous times for each classification by adjusting the kernel and gamma parameters, which determine the sensitivity of the classification, and visually assessing the classification within my training areas.

I conducted accuracy assessments for each classification by comparing each validation sample to the class of that same sample area on the thematic map. The accuracy assessment resulted in an error matrix for each classified map, with user's, producer's, and overall

accuracies, as well as Kappa coefficient values (Congalton and Green, 2019). Kappa is a measure of agreement between the classification and validation data, ranging from less than 0 (poor agreement) to 1 (almost perfect agreement) (Landis and Koch, 1977). The test statistic for Kappa analysis is a Z statistic, with a 95% confidence critical value of 1.96, in which case a classification can be considered significantly better than chance. Kappa coefficients were then compared between maps using the R 3.5 *irr* package (R Core Team, 2018; *v0.84.1*; Gamer *et al.*, 2019) to yield a Z statistic, which in this case indicates whether two error matrices are significantly different (Congalton and Green, 2019).

RESULTS

The most accurate classification across all image types, seasons, and classification methods was spring RGB imagery classified with OBIA (Figure 4a-b, Table 1, Table 2). This classification was one of eight that had statistically significant Z statistics, but it was the only classification to achieve a Kappa greater than 0.61 (0.64), indicating “substantial agreement” between the classification and validation data (Table 1; Landis and Koch, 1977). The spring RGB PBC classification had the second highest overall accuracy and significant Kappa (Fig. 4c-d, Table 1, Table 3). The only classifications that did not achieve a significant kappa ($Z > 1.96$) were those resulting from fall RGB imagery (Table 1). Fall MSP OBIA and fall MSP PBC were statistically significant (Kappa = 0.39, 0.32), whereas fall RGB OBIA and fall RGB PBC were not (Table 1). Overall accuracies calculated using the *B. thunbergii*, *R. multiflora*, and *Other* classes were below 40% (Table B1), with the exception of fall RGB with OBIA classification (overall accuracy = 65.30%), therefore all comparisons were conducted with the combined *Invasive* class.

Table 2: Comparison of overall (OA), user's (UA), and producer's accuracy (PA) for the *Invasive* class in each thematic map, with Kappa statistics, Z statistics, and p-values. Rows with significant Kappa statistics are in **bold**.

Classification	Season	Sensor	OA	UA	PA	Kappa	z	p
OBIA	Spring	MSP	69.44	80.00	60.00	0.40	3.53	4.00e⁻⁴
OBIA	Spring	RGB	82.35	80.95	89.47	0.64	5.29	1.21e⁻⁰⁷
OBIA	Fall	RGB	59.72	58.21	97.50	0.11	1.66	0.097
OBIA	Fall	MSP	70.83	69.39	85.00	0.39	3.45	0.001
PBC	Spring	MSP	70.83	67.27	92.50	0.38	3.60	3.00e⁻⁴
PBC	Spring	RGB	76.47	84.38	71.05	0.53	4.46	8.14e⁻⁰⁶
PBC	Fall	RGB	59.72	59.02	90.00	0.13	1.39	0.164
PBC	Fall	MSP	68.06	64.91	92.50	0.32	3.11	0.002

Table 3: Error matrix comparing spring RGB OBIA classification to validation reference data.

		Reference Data		User's Accuracy	
		Invasive	Other		
Map Data	Invasive	34	8	80.95%	
	Other	4	22	84.62%	
Producer's Accuracy		89.47%	73.33%	82.35%	Overall Accuracy

Table 4: Error matrix comparing spring RGB PBC classification to validation reference data.

		Reference Data		User's Accuracy	
		Invasive	Other		
Map Data	Invasive	27	5	84.38%	
	Other	11	25	69.44%	
Producer's Accuracy		71.05%	83.33%	76.47%	Overall Accuracy

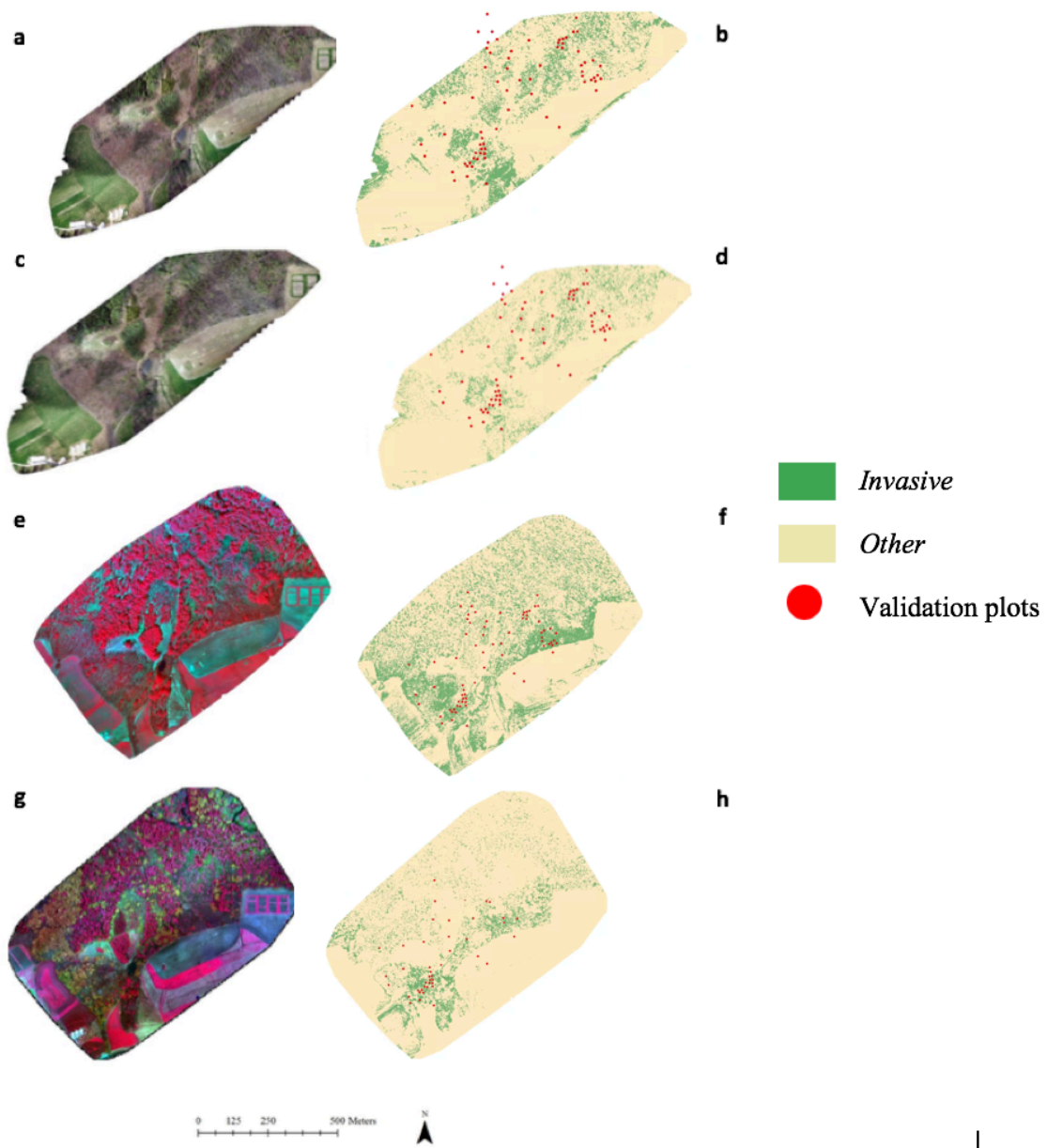


Figure 4: Imagery of study area and corresponding classifications a) from 5/04/2018 imagery with RGB sensor, b) OBIA classification of the 5/04/18 RGB imagery, c) from 5/04/2018 imagery with RGB sensor, d) PBC classification of the 5/04/18 imagery, e) from 4/23/18 imagery collected using MSP sensor, f) OBIA classification of 4/23/18 MSP imagery, g) from 11/09/18 MSP imagery and, h) OBIA classification of 11/9/18 MSP imagery.

Spring classifications overall outperformed fall classifications. Both spring RGB OBIA and spring RGB PBC were significantly better than their fall counterparts, fall RGB OBIA ($Z = 3.71$) and fall RGB PBC ($Z = 2.82$; Table 4). Spring classifications on average had higher kappa values than fall classifications (Table 4). No sensor type was universally superior. Fall MSP OBIA (Kappa = 0.39, OA = 70.83%) was the only classification to perform significantly better ($Z = 1.99$) than its RGB counterpart (Fall RGB OBIA, Kappa = 0.11, OA = 59.72%, Table 4). There were no significant differences between any spring RGB and spring MSP classifications. OBIA classification methods outperformed PBC methods in terms of average Kappa values and overall accuracies (Table 1), but there were no significant differences between spring RGB OBIA and spring RGB PBC, spring MSP OBIA and spring MSP PBC, or Fall RGB OBIA and Fall RGB PBC (Table 4).

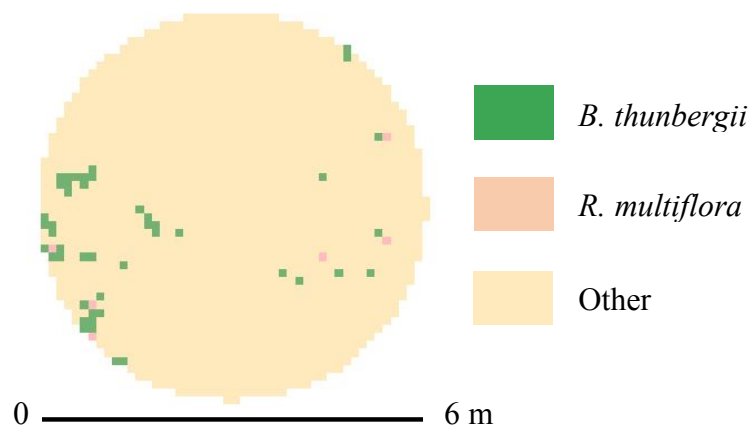


Figure 5: Example of an *Other* plot, totaling 28.27 m² in area. Despite the inclusion of both *Other* and *Invasive* pixels within the plot, there are not enough *Invasive*-labeled pixels to exceed the 1 m² MMU threshold. Therefore, the plot is correctly labelled as *Other*. The *Invasive* class includes both *B. thunbergii* and *R. multiflora* pixels.

Table 5: Pairwise comparison of error matrices represented by the Z statistic, generated through Kappa analysis between each pair of error matrices. Statistically significant Z statistics are in **bold**. Overall accuracy for each classification is reported on the diagonal in parentheses.

	Spring MSP OBIA	Spring RGB OBIA	Fall RGB OBIA	Fall MSP OBIA	Spring MSP PBC	Spring RGB PBC	Fall RGB PBC	Fall MSP PBC
Spring MSP OBIA	(69.44)							
Spring RGB OBIA	1.423	(82.35)						
Fall RGB OBIA	2.092	3.705	(59.72)					
Fall MSP OBIA	0.085	1.504	1.984	(70.83)				
Spring MSP PBC	0.180	1.647	1.987	0.092	(70.83)			
Spring RGB PBC	0.803	0.609	2.975	0.884	1.006	(76.47)		
Fall RGB PBC	2.002	3.495	0.121	1.904	1.893	2.822	(59.72)	
Fall MSP PBC	0.395	1.867	1.749	0.305	0.222	1.221	1.674	(68.06)

DISCUSSION

UAS collected imagery yielded classified maps that were up to 82% accurate, comparable to previous studies classifying invasive species using UAS imagery in open canopy habitats (Komarek et al., 2018; Mullerova et al., 2017a,b). Spring RGB imagery resulted in maps significantly more accurate than fall RGB imagery, regardless of classification method. *Berberis thunbergii* and *Rosa multiflora* were chosen for this study due to their tendency to leaf out early in spring, and the imagery reflected asynchronous phenology with canopy trees. High spring classification accuracies are consistent with previous remote sensing studies that took advantage of early spring green up to map widespread understory invasive species using satellite imagery (Becker et al., 2013; Singh et al., 2018; Wilfong et al., 2009) and are the first to demonstrate how well invasive plants in forest understory can be detected with UAS imagery.

My success in identifying invasive species from certain imagery has strong implications for UAS as an invasive management tool, with some caveats. In early May, *B. thunbergii* and *R. multiflora* were well into leaf elongation phase, while most native species were still in bud form or just breaking bud. This asynchrony in phenology was expected since both species are known to leaf out very early, but the visual distinction between native and invasive species was even more obvious than anticipated. The distinct differences in green vs no green in the understory allowed for confident training data selection by the analyst through manual image interpretation, but this was not the case for the fall imagery. Selecting training data in the fall imagery was very difficult due to both canopy and understory phenological status. Oak species held their leaves long into the fall, which was anticipated, blocking the view of species below. In addition, visible leaf litter closely resembled senescing *B. thunbergii* and *R. multiflora* leaves, which for *R. multiflora* was unexpected since it is cited to senesce late in autumn, and its stems are semi-

evergreen (Dlugos et al., 2015). Fall multi-temporal imagery can improve understory invasive classification (Resasco *et al.*, 2007; Shouse *et al.*, 2013), but due to technological difficulties, I was only able to collect one date of fall imagery. Anecdotally, honeysuckle (*Lonicera spp.*) and glossy buckthorn (*Frangula alnus*) remained green into November, and may be apparent within the imagery. Both of these invasive species are known for their autumn extended leaf phenology (Fridley, 2012), and have been mapped using non-UAS remote sensing methods (Resasco *et al.*, 2007; Becker *et al.*, 2013). The relative differences in canopy and understory species phenology indicates that collecting optimal understory UAS imagery is species specific and depends on knowing the dominant canopy composition of the intended area.

There were no significant differences overall between RGB and MSP sensors, although MSP imagery was required in fall to obtain significant classification results. RGB imagery yielded the highest spring classification accuracies and the three best classifications overall. The spatial resolution of the RGB imagery was greater than the MSP (3 cm as opposed to 13 cm), which qualitatively made the imagery easier to interpret and select training data. The majority of invasive plant remote sensing studies focus on multispectral satellite imagery (Bradley, 2014), though some have used RGB aerial and UAS imagery (Hill et al., 2017; Müllerová et al., 2017, 2013). MSP sensors are generally more expensive than RGB sensors, so high classification accuracies with an RGB sensor is promising for UAS as a cost-effective management tool. The blue wavelengths in RGB imagery can also penetrate shadows, which are almost inevitable in understory settings (Jensen, 2016). Many MSP sensors, such as the Sequoia I used, lack sensitivity to blue wavelengths, which increases the difficulty of classifying in and around shadows. Regardless of sensor, the optimal flying conditions are a calm day with consistently overcast sky, which removes or minimizes shadows, and results in a more even illumination.

Results indicated that OBIA classification does not achieve higher accuracies than PBC, contrary to the increasing literature recommending OBIA for UAS and high resolution image classification (Blaschke, 2010; Komarek et al., 2018; Mafanya et al., 2017). There was no significant difference between the spring RGB OBIA classification, which did have the highest overall accuracy, and any PBC classification other than Fall RGB PBC, which performed very poorly. OBIA classification is a commonly used classification method, particularly with UAS imagery (Komarek *et al.*, 2018; Mullerova *et al.*, 2017b; Singh and Frazier, 2018), but PBC may still be suitable for understory invasive mapping. Qualitative assessment of the imagery indicated that during orthomosaic creation, understory pixels can become blurred, resulting in less distinct shapes. In such a case, PBC may be advantageous since it only relies on spectral characteristics, whereas OBIA methods may get confused by branches overlaying invasive patches with indistinct margins. Furthermore, like MSP sensors, OBIA image analysis software such as eCognition is expensive, and requires more training than PBC methods before an analyst can effectively use it. Open source PBC classification programs such as Multispec (Purdue Research Foundation, 2019) are simple and require little training, which could increase the application of UAS by land managers or even private land owners.

Classifications could not distinguish between *B. thunbergii* and *R. multiflora*, leading them to be grouped into one *Invasive* class for analyses. There are a number of possibilities for this spectral confusion, the largest being that training data was limited and taken from one area in the imagery. It is generally recommended to take training samples from across the extent of the study area (Congalton and Green, 2019), but I chose to focus the *Invasive* training samples from one known area to better mimic how this technology would realistically be applied for land management. Another possibility for spectral confusion, particularly in the spring RGB imagery,

is the presence of inconsistent illumination across the study area over the course of the flight. Some sections of the orthomosaic were noticeably collected under cloud cover, while others are brightly illuminated. MSP sensors can remedy this issue since they incorporate a sunlight sensor, allowing for radiometric calibration so that the resulting orthomosaic is more uniformly calibrated than with an RGB sensor. However, while being able to distinguish between different invasive species would be ideal for prioritizing management, the distinction of the invasive species from the natives was successful and the ultimate priority of this study.

Other factors to consider for the applicability of UAS to invasive species management are user's and producer's accuracies. With respect to the *Invasive* class, user's accuracies indicate errors of commission, or false positives, while producer's accuracies indicate omission errors, or false negatives (Congalton and Green, 2019). When modelling invasive plant distributions, a low omission error (high producer's accuracy) is more important than a low commission error (high user's accuracy), meaning a false positive is less critical than a false negative (Ward, 2007). For instance, labelling an area with no invasive plants as *Invasive* is preferable to falsely labelling an invaded area as being uninvaded, because the species could be overlooked and continue to spread further. However, large numbers of false positives are undesirable as well, since the purpose of remote sensing for management is to focus and prioritize ground efforts. Spring MSP OBIA had a moderately high user's accuracy (80%), but a low producer's and overall accuracy (60% and 69%), meaning there were few false positives but many *Invasive* plots incorrectly labelled as *Other*. Conversely, spring RGB PBC 0.01 m² had a high producer's accuracy (100%), but a lower user's accuracy (68%), meaning that areas were frequently labelled both correctly and incorrectly as invasive. The commission errors found in spring RGB PBC are preferable to having higher omission errors, but there may be applications where the opposite may be more

helpful for management. For example, if a classification falsely labels nearly an entire property as invasive, that classification is not helpful for prioritizing management.

There are a number of improvements that could be made to this study. The investigation was approached as a proof of concept study, with the main goal to answer the overarching question of feasibility. The most obvious improvement would be to collect more data and across a larger study area or numerous properties. Having more training and validation data would allow for a more statistically robust study. Testing for optimal flight parameters would also likely improve results. A limited window for data collection, one spring and one fall, did not leave room for fine-tuning flying heights, spatial resolutions, and orthomosaic qualities. Multiple dates of imagery each season could also be used in a multi-temporal analysis, which, has increased classification accuracies in other invasive remote sensing studies (Resasco et al., 2007; Becker et al., 2013). Furthermore, I only used one OBIA machine learning algorithm, and one PBC algorithm per season. Other UAS studies have used numerous algorithms (Komarek *et al.*, 2018; Mullerova *et al.*, 2017b) to determine the best classification for a specific date of imagery, so it is possible that there are more suitable classifications that could be used.

A last aspect of UAS remote sensing not explored in this study is the use of classified point clouds. Through Structure from Motion, achieved by taking images of a single area from numerous angles, photogrammetric point clouds can be built using software such as Pix4D or Agisoft (St. Petersburg, Russia). These point clouds are not a substitute for Lidar, but they do have elevation and spectral data attached to each point, which can be separated into ground, canopy, and subcanopy. Leduc and Knudby (2018) successfully used a classified point cloud to map a native understory species prior to canopy leaf out by first separating out the canopy points. *Berberis thunbergii* and *R. multiflora* are both plants that grow low enough to the ground that

they may be easily separable from the canopy and also the ground. Furthermore, *R. multiflora* typically grows taller than *B. thunbergii*, which could aid in distinguishing the two from one another. In early spring, point cloud classification could be very helpful in distinguishing green understory plants from green canopy leaves.

I have shown that invasive understory plants can be classified using both RGB and MSP sensors, as well as PBC and OBIA classification. RGB imagery achieved higher classification accuracies than MSP imagery in spring, which has implications for invasive plant management applications, because RGB sensors are less expensive and more common in basic UAS kits. Accuracies over 70% were possible in fall if a MSP sensor was used, but collecting spring RGB imagery would be less costly and more accurate. While some individual OBIA classifications outperformed some individual PBC classifications, and vice versa, there was no clear classification method winner. The two classifications with the highest overall accuracies were spring RGB OBIA and spring RGB PBC, with no significant difference. OBIA does not necessarily increase classification accuracy, and effective maps for invasive plant management can be created using simple PBC classifications. Considering the lesser expense of RGB sensors and accessibility of open-source PBC software, UAS are a promising tool for invasive plant mapping.

REFERENCES

- Allan, B.F., Dutra, H.P., Goessling, L.S., Barnett, K., Chase, J.M., Marquis, R.J., Pang, G., Storch, G.A., Thach, R.E., Orrock, J.L., 2010. Invasive honeysuckle eradication reduces tick-borne disease risk by altering host dynamics. *Proc. Natl. Acad. Sci.* 107, 18523–18527.
- Allen, J.M., Bradley, B.A., 2016. Out of the weeds? Reduced plant invasion risk with climate change in the continental United States. *Biol. Conserv.* 203, 306–312.
- Allen, J.M., Leininger, T.J., Hurd, J.D., Civco, D.L., Gelfand, A.E., Silander, J.A., 2013. Socioeconomics drive woody invasive plant richness in New England, USA through forest fragmentation. *Landsc. Ecol.* 28, 1671–1686.
- Baatz, M., Schäpe, A., 2000. Multiresolution Segmentation: An Optimization Approach for High Quality Multi-scale Image Segmentation, in: *Angewandte Geographische Informationsverarbeitung XII, Beiträge Zum AGIT Symposium*. pp. 12–23.
- Ballard, M., Hough-Goldstein, J., Tallamy, D., 2013. Arthropod Communities on Native and Nonnative Early Successional Plants. *Environ. Entomol.* 42, 851–859.
- Becker, R.H., Zmijewski, K.A., Crail, T., 2013. Seeing the forest for the invasives: Mapping buckthorn in the Oak Openings. *Biol. Invasions* 15, 315–326.
- Binggeli, P., 2001. The human dimensions of invasive woody plants, in: *The Great Reshuffling: Human Dimensions of Invasive Alien Species*. pp. 145–159. J. McNeely. Cambridge, UK: IUCN.
- Blaschke, T., 2010. Object based image analysis for remote sensing. *ISPRS J. Photogramm. Remote Sens.* 65, 2–16.
- Bois, S.T., Silander, J.A., Mehrhoff, L.J., 2011. Invasive Plant Atlas of New England: The Role of Citizens in the Science of Invasive Alien Species Detection. *Bioscience* 61, 763–770.
- Bradley, B.A., 2014. Remote detection of invasive plants: A review of spectral, textural and phenological approaches. *Biol. Invasions* 16, 1411–1425.
- Bradley, B.A., Mustard, J.F., 2006. Characterizing the Landscape Dynamics of an Invasive Plant and Risk of Invasion Using Remote Sensing. *Ecol. Appl.* 16, 1132–1147.
- Brothers, T.S., Spingarn, A., Biology, S.C., Mar, N., 2009. Society for Conservation Biology Forest Fragmentation and Alien Plant Invasion of Central Indiana Old-Growth Forests. *Conserv. Biol.* 6, 91–100.
- Burges, C.J.C., 1998. A Tutorial on Support Vector Machines for Pattern Recognition. *Data Min. Knowl. Discov.* 2, 121–167.

- Christen, D.C., Matlack, G.R., 2009. The habitat and conduit functions of roads in the spread of three invasive plant species. *Biol. Invasions* 11, 453–465.
- Congalton, R., Green, K., 2019. *Assessing the Accuracy of Remotely Sensed Data: Principles and Practices*, 3rd ed. CRC Press, Boca Raton, FL.
- Dandois, J.P., Ellis, E.C., 2013. High spatial resolution three-dimensional mapping of vegetation spectral dynamics using computer vision. *Remote Sens. Environ.* 136, 259–276.
- Derraik, J., 2007. *Heracleum mantegazzianum* and *Toxicodendron succedaneum*: plants of human health significance in New Zealand and the National Pest Plant Accord. *N. Z. Med. J.* 120, 34–46.
- Dlugos, D.M., Collins, H., Bartelme, E.M., Drenovsky, R.E., 2015. The non-native plant *Rosa multiflora* expresses shade avoidance traits under low light availability. *Am. J. Bot.* 102, 1323–1331.
- Drăguț, L., Csillik, O., Eisank, C., Tiede, D., 2014. Automated parameterisation for multi-scale image segmentation on multiple layers. *ISPRS J. Photogramm. Remote Sens.* 88, 119–127.
- Dreiss, L.M., Volin, J.C., 2013. Forest Ecology and Management Influence of leaf phenology and site nitrogen on invasive species establishment in temperate deciduous forest understories. *For. Ecol. Manage.* 296, 1–8.
- Duro, D.C., Franklin, S.E., Dubé, M.G., 2012. Multi-scale object-based image analysis and feature selection of multi-sensor earth observation imagery using random forests. *Int. J. Remote Sens.* 33, 4502–4526.
- Ehrenfeld, J.G., 2003. Effects of Exotic Plant Invasions on Soil Nutrient Cycling Processes. *Ecosystems* 6, 503–523.
- Ehrenfeld, J.G., 1997. Invasion of Deciduous Forest Preserves in the New York Metropolitan Region by Japanese Barberry (*Berberis thunbergii* DC.). *J. Torrey Bot. Soc.* 124, 210–215.
- Eiswerth, M.E., Darden, T.D., Johnson, W.S., Agapoff, J., Harris, T.R., 2005. Input-Output Modeling, Outdoor Recreation, and the Economic Impacts of Weeds. *Weed Sci.* 53, 130–137.
- Elias, S.P., Lubelczyk, C.B., Rand, P.W., Lacombe, E.H., Holman, M.S., Smith, R.P., 2006. Deer browse resistant exotic-invasive understory: an indicator of elevated human risk of exposure to *Ixodes scapularis* (Acari: Ixodidae) in southern coastal Maine woodlands. *J. Med. Entomol.* 43, 1142–52.
- Evans, J.E., n.d. A literature review of management practices for multiflora rose (*Rosa multiflora*). *Nat. Areas J.* 3, 6–15.
- Executive Order 13112, 1999. Executive Order 13112 of February 3, 1999, Federal Register. United States.

- Fagan, M.E., Peart, D.R., 2004. Impact of the invasive shrub glossy buckthorn (*Rhamnus frangula* L.) on juvenile recruitment by canopy trees. *For. Ecol. Manage.* 194, 95–107.
- Farnsworth, E., 2004. Patters of Plant Invasions at Sites with Rare Plant Species Throughout New England. *Rhodora* 106, 97–117.
- Flory, S.L., Clay, K., 2006. Invasive shrub distribution varies with distance to roads and stand age in eastern deciduous forests in Indiana, USA. *Plant Ecol.* 184, 131–141.
- Fraser, B.T., Congalton, R.G., 2018. Issues in Unmanned Aerial Systems (UAS) data collection of complex forest environments. *Remote Sens.* 10, 908.
- Fridley, J.D., 2012. Extended leaf phenology and the autumn niche in deciduous forest invasions. *Nature* 485, 359–362.
- Gamer, M., Lemon, J., Fellows, I., Singh, P., 2019. irr: Various Coefficients of Interrater Reliability and Agreement. R package version 0.84.1. <https://cran.r-project.org/package=irr>
- Gao, Y., Mas, J.F., Kerle, N., Navarrete Pacheco, J.A., 2011. Optimal region growing segmentation and its effect on classification accuracy. *Int. J. Remote Sens.* 32, 3747–3763.
- Graff, L., 2006. Declining Profit Margin: When Volunteers Cost More Than They Return. *Int. J. Volunt. Adm.* XXIV, 47–56.
- Grybas, H., Melendy, L., Congalton, R.G., 2017. A comparison of unsupervised segmentation parameter optimization approaches using moderate- and high-resolution imagery. *GIScience Remote Sens.* 54, 515–533.
- Heberling, J.M., Fridley, J.D., 2013. Resource-use strategies of native and invasive plants in Eastern North American forests. *New Phytol.* 200, 523–533.
- Hejda, M., Pyšek, P., Jarošík, V., 2009. Impact of invasive plants on the species richness, diversity and composition of invaded communities. *J. Ecol.* 97, 393–403.
- Herron, P.M., Martine, C.T., Latimer, A.M., Leicht-Young, S.A., 2007. Invasive plants and their ecological strategies: Prediction and explanation of woody plant invasion in New England. *Divers. Distrib.* 13, 633–644.
- Hill, D.J., Tarasoff, C., Whitworth, G.E., Baron, J., Bradshaw, J.L., Church, J.S., 2017. Utility of unmanned aerial vehicles for mapping invasive plant species: a case study on yellow flag iris (*Iris pseudacorus* L.). *Int. J. Remote Sens.* 38, 2083–2105.
- Huebner, C.D., Steinman, J., Hutchinson, T.F., Ristau, T.E., Royo, A.A., 2014. The distribution of a non-native (*Rosa multiflora*) and native (*Kalmia latifolia*) shrub in mature closed-canopy forests across soil fertility gradients. *Plant Soil* 377, 259–276.
- Hulme, P.E., 2006. Beyond control: Wider implications for the management of biological invasions. *J. Appl. Ecol.* 43, 835–847.

- Husson, E., Ecke, F., Reese, H., 2016. Comparison of manual mapping and automated object-based image analysis of non-submerged aquatic vegetation from very-high-resolution UAS images. *Remote Sens.* 8, 1–18.
- Jensen, J.R., 2016. *Introductory Digital Image Processing: A remote sensing perspective*, 4th ed. Pearson Education, Inc, 1900 E. Lake Ave, Glenview, IL.
- Jordan, R.C., Brooks, W.R., Howe, D. V., Ehrenfeld, J.G., 2012. Evaluating the performance of volunteers in mapping invasive plants in public conservation lands. *Environ. Manage.* 49, 425–434.
- Kim, M., Warner, T., Madden, M., S. Atkinson, D., 2011. Multi-scale GEOBIA with very high spatial resolution digital aerial imagery: Scale, texture and image objects. *Int. J. Remote Sens.* 32, 2825–2850.
- Komárek, J., Klouček, T., Prošek, J., 2018. The potential of Unmanned Aerial Systems: A tool towards precision classification of hard-to-distinguish vegetation types? *Int. J. Appl. Earth Obs. Geoinf.* 71, 9–19.
- Kosmala, M., Crall, A., Cheng, R., Hufkens, K., Henderson, S., Richardson, A.D., 2016. Season spotter: Using citizen science to validate and scale plant phenology from near-surface remote sensing. *Remote Sens.* 8, 1–14.
- Landis, J.R., Koch, G.G., 1977. The Measurement of Observer Agreement for Categorical Data. *Biometrics* 33, 159–174.
- Leduc, M.B., Knudby, A.J., 2018. Mapping wild leek through the forest canopy using a UAV. *Remote Sens.* 10, 70.
- Lefsky, M., Cohen, W., Parker, G., Harding, D., 2002. Lidar Remote Sensing for Ecosystem Studies. *Bioscience* 52, 19-30.
- Lehan, N.E., Murphy, J.R., Thorburn, L.P., Bradley, B.A., 2013. Accidental introductions are an important source of invasive plants in the continental United States. *Am. J. Bot.* 100, 1287–1293.
- Leung, B., Lodge, D.M., Finnoff, D., Shogren, J.F., Lewis, M.A., Lamberti, G., 2002. An ounce of prevention or a pound of cure: Bioeconomic risk analysis of invasive species. *Proc. R. Soc. B Biol. Sci.* 269, 2407–2413.
- Li, P., Jiang, L., Feng, Z., 2013. Cross-comparison of vegetation indices derived from landsat-7 enhanced thematic mapper plus (ETM+) and landsat-8 operational land imager (OLI) sensors. *Remote Sens.* 6, 310–329.
- Liao, C., Peng, R., Luo, Y., Zhou, X., Wu, X., Fang, C., Chen, J., Li, B., 2008. Altered ecosystem carbon and nitrogen cycles by plant invasion: A meta-analysis. *New Phytol.* 177, 706–714.

- Lillesand, T., Kiefer, R., Chipman, J., 2015. Remote Sensing and Image Interpretation, 7th ed. Wiley, Hoboken, NJ.
- Lommen, S.T.E., Jongejans, E., Leitsch-Vitalos, M., Tokarska-Guzik, B., Zalai, M., Müller-Schärer, H., Karrer, G., 2018. Time to cut: population models reveal how to mow invasive common ragweed cost-effectively. *NeoBiota* 39, 53–78.
- Lu, B., He, Y., 2017. ISPRS Journal of Photogrammetry and Remote Sensing Species classification using Unmanned Aerial Vehicle (UAV) -acquired high spatial resolution imagery in a heterogeneous grassland. *ISPRS J. Photogramm. Remote Sens.* 128, 73–85.
- Lu, D., Weng, Q., 2007. A survey of image classification methods and techniques for improving classification performance. *Int. J. Remote Sens.* 28, 823–870.
- Lym, R., Nelson, J., 2000. The Distribution of Leafy Spurge (*Euphorbia esula*) and Other Weedy *Euphorbia* spp . in the United States. *Weed Technol.* 14, 642–646.
- Mafanya, M., Tsele, P., Botai, J., Manyama, P., Swart, B., Monate, T., 2017. Evaluating pixel and object based image classification techniques for mapping plant invasions from UAV derived aerial imagery: *Harrisia pomanensis* as a case study. *ISPRS J. Photogramm. Remote Sens.* 129, 1-11.
- Martin, L.J., Blossey, B., 2012. Invasive plant cover impacts the desirability of lands for conservation acquisition. *Biodivers. Conserv.* 21, 1987–1996.
- Matlack, G.R., 1993. Microclimate variation within and among edge sites in the eastern United States. *Biol. Conserv.* 66, 185–194.
- Müllerová, J., Bartaloš, T., Brůna, J., Dvořák, P., Vítková, M., 2017a. Unmanned aircraft in nature conservation: an example from plant invasions. *Int. J. Remote Sens.* 38, 2177–2198.
- Müllerová, J., Bruna, J., Bartalos, T., Dvořák, P., Vítková, M., Pyšek, P., 2017b. Timing is Important: unmanned aircraft vs satellite imagery in plant invasion monitoring. *Front. Plant Sci.* 8, 887.
- Müllerová, J., Pergl, J., Pyšek, P., 2013. Remote sensing as a tool for monitoring plant invasions: Testing the effects of data resolution and image classification approach on the detection of a model plant species *Heracleum mantegazzianum* (giant hogweed). *Int. J. Appl. Earth Obs. Geoinf.* 25, 55–65.
- Nelson, C.A., Saha, S., Kugeler, K.J., Delorey, M.J., Shankar, M.B., Hinckley, A.F., Mead, P.S., 2015. Incidence of Clinician-Diagnosed Lyme Disease, United States, 2005-2010. *Emerg. Infect. Dis.* 21, 1625–1631.
- New Hampshire Code of Administrative Rules. 2004. [Invasive species, Chapter Agr. 3800](#) (15 September 2004). State of New Hampshire. URL <https://www.agriculture.nh.gov/publications-forms/documents/prohibited-invasive-species.pdf> (accessed 06.11.18)

- Olsson, A.D., van Leeuwen, W.J.D., Marsh, S.E., 2011. Feasibility of invasive grass detection in a desertscrub community using hyperspectral field measurements and landsat TM imagery. *Remote Sens.* 3, 2283–2304.
- Ostfeld, R.S., Brunner, J.L., 2015. Climate change and Ixodes tick-borne diseases of humans. *Philos. Trans. R. Soc. B* 370, 20140051.
- Otto, C., Nilsson, L., 1981. Why Do Beech and Oak Trees Retain Leaves Until Spring. *Oikos* 37, 387–390.
- Pimentel, D., Zuniga, R., Morrison, D., 2005. Update on the environmental and economic costs associated with alien-invasive species in the United States. *Ecol. Econ.* 52, 273–288.
- Pix4D, 2018. Pix4Dmapper 3.2 User Manual. Pix4D SA, Lausanne, Switzerland.
- Polgar, C., Gallinat, A., Primack, R.B., 2014. Drivers of leaf-out phenology and their implications for species invasions: Insights from Thoreau’s Concord. *New Phytol.* 202, 106–115.
- Powell, K.I., Chase, J.M., Knight, T.M., 2013. Invasive plants have scale-dependent species-area relationships. *Science* 339, 316–318.
- Pyšek, P., Jarošík, V., Hulme, P.E., Pergl, J., Hejda, M., Schaffner, U., Vilà, M., 2012. A global assessment of invasive plant impacts on resident species, communities and ecosystems: The interaction of impact measures, invading species’ traits and environment. *Glob. Chang. Biol.* 18, 1725–1737.
- Reichard, S.H., White, P., 2001. Horticulture as a Pathway of Invasive Plant Introductions in the United States. *Bioscience* 51, 103–113.
- Resasco, J., Hale, A.N., Henry, M.C., Gorchoy, D.L., 2007. Detecting an invasive shrub in a deciduous forest understory using latefall Landsat sensor imagery. *Int. J. Remote Sens.* 28, 3739–3745.
- Richardson, A.D., Bailey, A.S., Denny, E.G., Martin, C.W., O’Keefe, J., 2006. Phenology of a northern hardwood forest canopy. *Glob. Chang. Biol.* 12, 1174–1188.
- Richter, R., Berger, U.E., Dullinger, S., Essl, F., Leitner, M., Smith, M., Vogl, G., 2013. Spread of invasive ragweed: Climate change, management and how to reduce allergy costs. *J. Appl. Ecol.* 50, 1422–1430.
- Schirmel, J., Bundschuh, M., Entling, M.H., Kowarik, I., Buchholz, S., 2016. Impacts of invasive plants on resident animals across ecosystems, taxa, and feeding types: A global assessment. *Glob. Chang. Biol.* 22, 594–603.
- Shouse, M., Liang, L., Fei, S., 2013. Identification of understory invasive exotic plants with remote sensing in urban forests. *Int. J. Appl. Earth Obs. Geoinf.* 21, 525–534.

- Silander, J.A., Klepeis, D.M., 1999. The invasion ecology of Japanese barberry (*Berberis thunbergii*) in the New England landscape. *Biol. Invasions* 1, 189–201.
- Singh, K.K., Chen, Y.H., Smart, L., Gray, J., Meentemeyer, R.K., 2018. Intra-annual phenology for detecting understory plant invasion in urban forests. *ISPRS J. Photogramm. Remote Sens.* 142, 151–161.
- Singh, N., Glenn, N.F., 2009. Multitemporal spectral analysis for cheatgrass (*Bromus tectorum*) classification. *Int. J. Remote Sens.* 30, 3441–3462.
- Smith, L.M., 2013. Extended leaf phenology in deciduous forest invaders: Mechanisms of impact on native communities. *J. Veg. Sci.* 24, 979–987.
- USDA, 2019. Introduced, Invasive, and Noxious Plants [WWW Document]. NRCS Invasive Species Policy. URL <https://plants.usda.gov/java/noxiousDriver> (accessed 11.11.18).
- USGS, 2016. Landsat – Earth observation satellites: Fact Sheet [WWW Document]. URL <https://pubs.usgs.gov/fs/2015/3081/fs20153081.pdf> (accessed 6.11.18).
- Vilà, M., Espinar, J.L., Hejda, M., Hulme, P.E., Jarošík, V., Maron, J.L., Pergl, J., Schaffner, U., Sun, Y., Pyšek, P., 2011. Ecological impacts of invasive alien plants: A meta-analysis of their effects on species, communities and ecosystems. *Ecol. Lett.* 14, 702–708.
- Ward, D.F., 2007. Modelling the potential geographic distribution of invasive ant species in New Zealand. *Biol. Invasions* 9, 723–735.
- Ward, J.S., Williams, S.C., Linske, M.A., 2018. Influence of invasive shrubs and deer browsing on regeneration in temperate deciduous forests 67, 58–67.
- Wellings, C.R., 2011. Global status of stripe rust: A review of historical and current threats. *Euphytica* 179, 129–141.
- Westbrooks, R., 2004. New Approaches for Early Detection and Rapid Response to Invasive Plants in the United States Author. *Weed Sci.* 18, 1468–1471.
- Whitehead, K., Hugenholtz, C.H., 2014. Remote sensing of the environment with small unmanned aircraft systems (UASs), part 1: a review of progress and challenges. *J. Unmanned Veh. Syst.* 2, 69–85.
- Wilfong, B.N., Gorchov, D.L., Henry, M.C., 2009. Detecting an Invasive Shrub in Deciduous Forest Understories Using Remote Sensing. *Weed Sci.* 57, 512–520.
- Williams, S.C., Ward, J.S., Worthley, T.E., Stafford, K.C., 2009. Managing Japanese Barberry (*Ranunculales: Berberidaceae*) Infestations Reduces Blacklegged Tick (*Acari: Ixodidae*) Abundance and Infection Prevalence With *Borrelia burgdorferi* (*Spirochaetales: Spirochaetaceae*). *Environ. Entomol.* 38, 977–984.
- Yu, Q., Gong, P., Clinton, N., Biging, G., Kelly, M., Schirokauer, D., 2006. Object-based

Detailed Vegetation Classification with Airborne High Spatial Resolution Remote Sensing Imagery. *Photogramm. Eng. & Remote Sens.* 72, 799–811.

Yurkonis, K.A., Meiners, S.J., Wachholder, B.E., 2005. Invasion impacts diversity through altered community dynamics. *J. Ecol.* 93, 1053–1061.

APPENDIX A: Data Collection Details

Site Selection and Imagery

I chose Kingman Farm as the study area after analyzing previously collected vegetation data and confirming with ground surveys. The UNH College Woodlands Continuous Forest Inventory (CFI) dataset, updated approximately every 5 years to reflect changes in tree and understory vegetation in permanent plots, indicated that Kingman Farm, among other properties, had numerous areas with abundant invasive plant coverage. Through random haphazard surveys, I confirmed that Kingman Farm contained patches of dominant *B. thunbergii* and *R. multiflora* coverages. I visually estimated these patches to be 10 m² or larger and under deciduous and mixed canopies. The distribution of these two species was enough to designate several replicate areas, which distinguished Kingman Farm from other properties as an ideal study site. I marked all candidate invasive patches as I encountered them with a waypoint on a Garmin GPSMap76CS (Garmin, Olathe, KS; horizontal accuracy: 5-10 m; coordinate system: WGS84; WAAS enabled) over the course of five dates between February and July 2018. The property is also close to the University of New Hampshire's (UNH) Durham campus, which is necessary for traveling to the study site at short notice to take advantage of favorable flying conditions.

To ensure that I would not miss my phenological window, I monitored indicator plots of *B. thunbergii* and *R. multiflora* at anticipated periods of phenological change weekly early March through late May, and again in early October through mid-November. These indicator plots were located off-trail at Kingman Farm, in an easily accessible location but with light exposure that upon visual assessment appeared average to Kingman stands. I flagged one *B. thunbergii* and one *R. multiflora* shrub and monitored them for phenological changes. I tracked phenology using the established standards set by the National Phenology Network (USA National

Phenology Network, 2017), including phenophases of bud presence, budburst, leaf out, leaf elongation, flower bud presence, and open flowers. As changes occurred, I recorded them as a percentage of the individual shrub. For example, when my *B. thunbergii* tagged individual hit budburst, I described it as 40% budburst, with 60% unburst buds. I also tracked general phenological changes of canopy species in both early spring and late fall to assess levels of canopy leaf out and leaf off. Between 5/8/18 and 6/20/18 I continued flights in the chance that invasive shrub flowering was visible through canopy gaps. However, the canopy was too closed in to see the ground in the imagery in these dates and this imagery was not used in the final analysis.

Table A1: Phenology tracking sheet for invasive understory plants and canopy tree species.

Date	Spp	Buds (%)	Bud Break (%)	Emergent Leaves (%)	Leaf Unfolding (%)	Full Leaves (%)	Flower Buds	Open Flowers	Fruit	Ripe Fruit	Ripe Fruit Count	Leaf Coloration	Leaf Coloration (% green)	Leaf Drop	Leaf Drop (% remaining)	Notes

Recent UAS studies found that higher flying heights results in more successful image calibration and resulting orthomosaic creation (Fraser and Congalton, 2018). However, since my intent was to assess UAS as a tool for early invasion monitoring, I focused on collecting imagery that would yield the highest possible resolution, so that the smallest plant units possible could be classified. Lower flying heights did result in less than optimal orthomosaic creation, so I experimented with increasing flying height from 80m to 100m, which yielded better results. Another factor in determining flying heights was the specific UAS used. I collected the spring RGB imagery using the Eagle XF, which could safely fly at heights of 80m above the ground. However, after June 2018, I had to switch to using the eBee for both RGB and MSP imagery due

to technical difficulties. Due to a sensitive ground sensor system on the eBee, I had difficulty collecting imagery at 80m because the system thought it was too close to the tree canopy. Flying at 100 m resolved this issue and still resulted in very high resolution imagery.

I selected imagery to classify based on the relative phenology of the native tree species and *B. thunbergii* and *R. multiflora*. By studying the known training area where I had put out target points marking patches of the invasive species, it was straightforward to determine which date of imagery I could see the invasive species the best without being obscured by leafing out tree species in the spring. Since I only collected one date of fall imagery, I used what I had. Although I waited as long as possible for canopy leaf drop to advance, it was much more difficult to visually identify invasive species in the fall imagery due to their resemblance in color to fallen leaves.

Table A2: Date, UAS model, camera model, sensor type, and flying height of imagery collected in 2018. Sensors types are multispectral (MSP) and red-green-blue (RGB). Dates included in the main text are indicated in **bold**.

Date	UAS	Camera	Sensor Type	Flying Height (m)
4/12/18	EBee Plus	Sequoia	MSP	100 and 120
4/23/18	eBee Plus	Sequoia	MSP	100
5/4/18	Eagle XF	a7R	RGB	80
5/8/18	Eagle XF	a7R	RGB	80 and 120
5/23/18	EagleXF	a7R	RGB	80 and 120
6/4/18	Eagle XF	a7R	RGB	120
6/20/18	Eagle XF	a7R	RGB	120
11/9/18	EBee Plus	S.O.D.A, Sequoia	RGB, MSP	100 and 120

Vegetation Plot Sampling Details

I used 1 m² subplots to estimate the average density of *B. thunbergii* and *R. multiflora* using the following scale: <5, 5-25, 25-50, 50-75, 75-100. For *B. thunbergii*, the scale numbers refer to the number of lateral stems, while for *R. multiflora* I counted the number of compound leaves. I performed several calibration counts, but overall these were rough estimates to measure ordinal invasive density in the plot. Density assessments were separate for adult plants—those with woody stems—and “young shoots”, which were suckers or other non-woody first year growth. The distinction in plant age is pertinent because only adult stems are present and leafing in early spring, but young shoots could influence fall classification.

In addition to the vegetation composition and coverage measurements, I characterized the general distribution of *B. thunbergii* and *R. multiflora* in the 3m radius plot based on presence by quadrant—northeast, southeast, southwest, and northwest. This was presence/absence data only. For example, if *B. thunbergii* was present in the northeast and southeast quadrants, I recorded it as present in those two quadrants and absent in the others. If *R. multiflora* also happened to be in those same quadrants, that was recorded as well. I also recorded presence data for *Symplocarpus foetidus* (skunk cabbage) and *Frangula alnus* (glossy buckthorn). *Symplocarpus foetidus* was in an active growth state at the time early spring imagery was collected—as such, it was important to note in case of classification confusion in the imagery. *Frangula alnus* was another invasive plant species present in the study area that could also be confused with other early leaf-out vegetation. I classified ground type(s) as wet, bare, litter, rock, and/or grassy in case that interfered with imagery classification.

Table A3: Ground data plot sampling field sheet used to collect validation reference data.

Kingman Plot Sampling Data Sheet									
PlotID: _____					Date: _____				
GPS coordinates: _____					Weather: _____				
RTK HSDV: _____					Notes: _____				
Canopy Closure:		1: <5%	2: 5-25%	3: 25-50%	4: 50-75%	5: 75-100%			
Canopy Composition: _____									
Ground Type:		Bare	Litter	Wet	Rock				
Veg Height Categories: 1: <20cm 2: 20-100cm 3: 100-200cm 4: >200cm									
Topcon Plot ID	Total % Veg Cover	B.thunbergii Cover	B.thunbergii Avg Height	R.Multiflora Cover	R.Multiflora Avg Height	Shrub Cover, height	Fern Cover, height	Herb Cover, height	
B. thunbergii dist in plot	NE	SE	SW	NW	ALL	NA	Clumped	Even	
R. multiflora dist in plot	NE	SE	SW	NW	ALL	NA	Clumped	Even	
Subplot locs	1	2	3						
Az, dist									
Subplot	# B. thunbergii adult individuals	# B. thunbergii branches	# B. thunbergii young shoots	# R. multiflora adult individuals	# R. Multiflora adult compound leaves	# R. Multiflora young shoots	Shrub individuals	Fern individuals	Herb individuals
1									
2									
3									
Other Notes:									
Entered into Excel:									
Azimuths									

APPENDIX B: Species-Specific Accuracy Assessment Results

I first classified my imagery and ran accuracy assessments with *B. thunbergii* and *R. multiflora* as separate classes, but the overall accuracies were very low across all classifications, with the highest being Fall RGB OBIA at 65.31% overall accuracy. These low overall accuracies led to me combining the two species-level classes into one invasive class for accuracy assessment.

Table B1: Comparison of overall accuracy (OA), user's accuracy (UA), and producer's accuracy (PA) for classifications generated using separate *B. thunbergii* (barberry), *R. multiflora* (rose), and *Other* map classes. Sensor designations include red, green, blue (RGB) and multispectral (MSP). Object based image analysis (OBIA) is the second classification type.

Season	Sensor	Class.	OA	Barberry UA	Barberry PA	Rose UA	Rose PA
Spring	MSP	OBIA	0.33	0.30	0.14	0.33	0.28
Spring	RGB	OBIA	0.34	0.38	0.15	0.36	0.56
Fall	RGB	OBIA	0.65	0.67	0.64	0.58	0.83
Fall	MSP	OBIA	0.45	0.50	0.68	0.55	0.33
Spring	MSP	PBC	0.38	0.46	0.86	0.25	0.11
Spring	RGB	PBC	0.39	0.19	0.15	0.67	0.56
Fall	RGB	PBC	0.57	0.64	0.45	0.60	0.95
Fall	MSP	PBC	0.24	.24	0.23	0.32	0.44